KING'S BUSINESS SCHOOL

Data Analytics for Finance & Macro Research Centre

KING'S College LONDON

A Three-Dimensional Asymmetric Power HEAVY Model

S. Yfanti, G. Chortareas, M. Karanasos, E. Noikokyris

Working paper No. 2020/6 | September 2020 | ISSN 2516-5933

A Three-Dimensional Asymmetric Power HEAVY Model

S. Yfanti[†,*], G. Chortareas[‡], M. Karanasos[⋆], E. Noikokyris[⊛]

[†]*Loughborough University, UK;* [‡]*King's College London, UK;*

[⋆]*Brunel University London, UK;* [⊛]*Kingston University London, UK*

September 2020

Abstract

This paper proposes the three-dimensional HEAVY system of daily, intra-daily and range-based volatility equations. We augment the bivariate model with a third volatility metric, the Garman-Klass estimator, and enrich the trivariate system with power transformations and asymmetries. Most importantly, we derive the theoretical properties of the multivariate asymmetric power model and explore its finite-sample performance through a simulation experiment on the size and power properties of the diagnostic tests employed. Our empirical application shows that all three power transformed conditional variances are found to be significantly affected by the powers of squared returns, realized measure, and range-based volatility as well. We demonstrate that the augmentation of the HEAVY framework with the range-based volatility estimator, leverage and power effects improves remarkably its forecasting accuracy. Finally, our results reveal interesting insights for investments, market risk measurement, and policymaking.

Keywords: asymmetries, HEAVY model, high-frequency data, power transformations, realized volatility, risk management.

JEL classification: C22, C58, G01, G15

*Corresponding Author: Dr Stavroula Yfanti. School of Business and Economics, Loughborough University, Epinal Way, Loughborough, LE11 3TU, UK. Telephone: +44 (0)1509 227091. Email: stavyfan@gmail.com. ORCID ID: 0000-0001-8071-916X

1 Introduction

Financial volatility lies at the core of empirical finance research, with direct employment in investments, risk management practices, and financial stability oversight. Reliable modeling and accurate forecasting of the volatility pattern has been the main objective of financial applications for business operations, given that volatility is considered as one of the fundamental input variables in estimations and decision processes of any corporation on derivatives pricing, portfolio immunization, investment diversification, firm valuation, and funding choices. Financial volatility is also closely inspected by policymakers since it entails critical destabilizing threats for the financial system.

We develop a three-dimensional HEAVY[1] model by augmenting the bivariate system of Shephard and Sheppard (2010) with a third variable, namely, the range-based Garman-Klass volatility. Another contribution is the enrichment of the trivariate model with asymmetries and power transformations through the APARCH structure of Ding et al. (1993). Motivated by the established merits of this framework, which considerably improves Bollerslev's (1986) GARCH process by adding leverage and power effects (see, for example, Brooks et al., 2000, Karanasos and Kim, 2006), we similarly extend the trivariate system with these two features to explore its superiority over the benchmark specification. Most importantly, we derive the theoretical time series properties (optimal predictors and second moment structure) of the multivariate asymmetric power system and explore its finite-sample performance through a simulation experiment. We further proceed with an empirical application of the proposed model, to examine the various nested specifications in depth by investigating their performance over five stock indices. One of our key findings is that each of the three powered conditional variances is significantly affected by the first lags of all three power transformed variables, that is, squared negative returns, realized variance, and Garman-Klass volatility.

Following the burst of the 2008 crisis, when volatilities rose sharply and persistently with crucial systemic risk externalities, we witnessed a resurgence of regulators' and academics' interest in meaningful volatility estimates, while, at the same time, practitioners remained alert to improving the relevant volatility frameworks on a day-to-day basis. Financial economics scholars focused on volatility as a potent catalyst of systemic risk build-up, which policymakers tried to limit. We demarcate this study from the extant finance bibliography by extending the benchmark HEAVY model with asymmetries, power transformations, and Garman-Klass volatility providing a well-defined framework that adequately fits the volatility process. We further examine the theoretical properties of the proposed model and demonstrate its forecasting superiority over the benchmark specification using a rolling window out-of-sample forecasting procedure. The three-dimensional system of volatility equations, we establish, is ready-to-use,

[1] The acronym HEAVY is derived by 'High-frEquency-bAsed VolatilitY' in Shephard and Sheppard (2010).

not only on stock market returns but also on further asset classes or financial instruments (exchange rate, cryptocurrency, commodity, real estate, and bond returns) and multiple financial economics applications of business operations, such as bonds investing, foreign exchange trading and commodities hedging, core daily functions in the treasuries of most financial and non-financial corporations.

Overall, our proposed volatility modeling framework improves the HEAVY model, with important implications for market practitioners and policymakers on forecasting the trajectory of the financial returns' second moment. Volatility modeling and forecasting are essential for asset allocation, pricing, and risk hedging strategies. A reliable volatility forecast, exploiting in full the high-frequency domain, is the input variable of paramount importance for the processes of derivatives pricing, effective cross-hedging, Value-at-Risk measurement, investment allocation, and portfolio optimization with different asset classes and financial instruments. Moreover, the robust volatility modeling approach we introduce provides a useful tool not only for market players but also for policymakers. Policymaking includes continuous oversight duties and prudential regulation practices. In this vein, it is imperative for the authorities to account for the volatility of financial markets across every aspect of the financial system's policy responses, both post-crisis through stabilization policy reactions and pre-crisis through proactive assessment of financial risks. The asymmetric power HEAVY framework we propose here has been shown to perform significantly better than the benchmark specification both in the short- and long-term forecasting horizons. Trading and risk management processes mostly use one- to ten-day forecasts while policymakers are involved in longer-term predictions of financial volatility. Hence, we illustrate our model's forecasting superiority with a Value-at-Risk example that provides both risk management and policy implications.

The remainder of the paper is structured as follows. In Section 2 we detail the three-dimensional HEAVY formulation and our extension, which allows for asymmetries and power transformations. Section 3 introduces the theoretical properties of the multivariate asymmetric power HEAVY model and contains a simulation experiment on the finite-sample properties of the diagnostic tests employed. Section 4 describes the data and presents the results of the empirical application of the asymmetric power specification. In Section 5, we calculate multiple-step-ahead forecasts to measure the out-of-sample performance of the proposed specifications. Finally, Section 6 concludes the analysis.

2 The HEAVY Framework

There are several studies introducing non-parametric estimators of realized volatility using high-frequency market data. Andersen and Bollerslev (1998), Andersen et al. (2001) and Barndorff-Nielsen and Shephard (2002) were the first that econometrically formalized the realized variance with quadratic variation-like

measures, while Barndorff-Nielsen et al. (2008, 2009) focused on the realized kernel estimation as a realized measure which is more robust to noise.

A large body of empirical research focuses on modeling and forecasting the realized volatility. Various studies combine it with the conditional variance of returns. Engle (2002b) proposed the GARCH-X process, where the former is included as an exogenous variable in the equation of the latter. Corsi et al. (2008) suggested the HAR-GARCH formulation for modeling the volatility of realized volatility. Hansen et al. (2012) introduced the Realized GARCH model that corresponds more closely to the HEAVY framework of Shephard and Sheppard (2010), which jointly estimates conditional variances based on both daily (squared returns) and intra-daily (it uses the realized measure - kernel and variance - as a measure of ex-post volatility) data, so that the system of equations adopts to information arrival more rapidly than the classic daily GARCH process. One of its advantages is the robustness to certain forms of structural breaks, especially during the crisis periods, since the mean reversion and short-run momentum effects result in higher quality performance in volatility level shifts and more reliable forecasts. Borovkova and Mahakena (2015) employed a HEAVY specification with a skewed-t error distribution, while Huang et al. (2016) incorporated the HAR structure of the realized measure in the GARCH conditional variance specification in order to capture the long memory of the volatility dynamics.

The benchmark HEAVY model of Shephard and Sheppard (2010) can be extended in many directions. We allow for power transformations and leverage effects in the conditional variance process to improve volatility modeling and forecasting further (see also the Supplementary Appendix on the enrichment of the trivariate asymmetric power specification with long memory features and structural breaks).

2.1 Benchmark Model

The HEAVY model uses two variables: the close-to-close stock returns (r_t) and the realized measure of variation based on high-frequency data, RM_t. We first form the signed square rooted (SSR) realized measure as follows: $\widetilde{RM_t} = sign(r_t)\sqrt{RM_t}$, where $sign(r_t) = 1$, if $r_t \geqslant 0$ and $sign(r_t) = -1$, if $r_t < 0$.

In this paper we test the inclusion of an alternative measure of volatility to the HEAVY framework, that is we employ the classic range-based estimator of Garman and Klass (1980), hereafter GK. We further form the SSR GK volatility ($\widetilde{GK}_t = sign(r_t)\sqrt{GK_t}$).

We assume that the returns, the SSR realized measure and GK volatility are characterized by the following relations:

$$r_t = e_{rt}\sigma_{rt},\ \widetilde{RM_t} = e_{Rt}\sigma_{Rt},\ \widetilde{GK}_t = e_{gt}\sigma_{gt}, \tag{1}$$

where the stochastic term e_{it} is independent and identically distributed ($i.i.d$), $i = r, R, g$; σ_{it} is positive with probability one for all t and it is a measurable function of $\mathcal{F}_{t-1}^{(XF)}$, that is the filtration generated

by all available information through time $t-1$. We will use $\mathcal{F}_{t-1}^{(HF)}$ $(X = H)$ for the high-frequency past data, i.e., for the case of the realized measure, or $\mathcal{F}_{t-1}^{(LoF)}$ $(X = Lo)$ for the low-frequency past data, i.e., for the case of the close-to-close returns. Hereafter, for notational convenience, we will drop the superscript XF.

In the HEAVY/GARCH model e_{it} has zero mean and unit variance. Therefore, the three series have zero conditional means, and their conditional variances are given by

$$\mathbb{E}(r_t^2\,|\mathcal{F}_{t-1}) = \sigma_{rt}^2,\ \mathbb{E}(\widetilde{RM_t}^2\,|\mathcal{F}_{t-1}) = \mathbb{E}(RM_t\,|\mathcal{F}_{t-1}) = \sigma_{Rt}^2, \text{ and } \mathbb{E}(\widetilde{GK_t}^2\,|\mathcal{F}_{t-1}) = \mathbb{E}(GK_t\,|\mathcal{F}_{t-1}) = \sigma_{gt}^2, \tag{2}$$

where $\mathbb{E}(\cdot)$ denotes the expectation operator. The three equations are called HEAVY-i, $i = r, R, g$ for the returns, the realized measure, and Garman Klass volatility, respectively.

2.2 Asymmetric Power Formulation

The asymmetric power (AP) specification for the three-dimensional (3D) HEAVY$(1,1)$ consists of the following equations (in what follows for notational simplicity, we will drop the order of the model if it is $(1,1)$):

$$(1-\beta_i L)(\sigma_{it}^2)^{\frac{\delta_i}{2}} = \omega_i + (\alpha_{ir}+\gamma_{ir}s_{t-1})L(r_t^2)^{\frac{\delta_r}{2}} + (\alpha_{iR}+\gamma_{iR}s_{t-1})L(RM_t)^{\frac{\delta_R}{2}} + (\alpha_{ig}+\gamma_{ig}s_{t-1})L(GK_t)^{\frac{\delta_g}{2}}, \tag{3}$$

where L is the lag operator, $\delta_i \in \mathbb{R}_{>0}$ (the set of the positive real numbers) are the power parameters, for $i = r, R, g$, and $s_t = 0.5[1-sign(r_t)]$, that is, $s_t = 1$ if $r_t < 0$ and 0 otherwise; γ_{ii}, γ_{ij} $(i \neq j)$ are the own and cross leverage parameters, respectively[2]; positive γ_{ii}, γ_{ij} means larger contribution of negative 'shocks' in the volatility process (in our long memory AP specification we will replace $\alpha_{ii} + \gamma_{ii}s_{t-1}$ by $\alpha_{ii}(1+\gamma_{ii}s_{t-1})$; see the Supplementary Appendix, eq. (1)). In this specification the powered conditional variance, $(\sigma_{it}^2)^{\delta_i/2}$, is a linear function of the lagged values of the power transformed squared returns, realized measure and GK volatility.

We will distinguish between three different asymmetric cases: the double one (DA: $\gamma_{ij} \neq 0$ for all i and j) and two more, own asymmetry (OA: $\gamma_{ij} = 0$ for $i \neq j$ only) and cross asymmetry (CA: $\gamma_{ii} = 0$).

The α_{iR} and γ_{iR} are called the (six) Heavy parameters (own when $i = R$ and cross when $i \neq R$). These parameters capture the impact of the realized measure on the three conditional variances. Similarly, the α_{ir} and γ_{ir} (six in total) are called the Arch parameters (own when $i = r$ and cross for $i \neq r$). They depict the influence of the squared returns on the three conditional variances. Finally, the α_{ig} and γ_{ig} are called the (six) Garman parameters. These parameters capture the effects of the GK volatility on the three conditional variances.

[2] This type of asymmetry was introduced by Glosten et. al. (1993).

The asymmetric power model is equivalent to a trivariate AP-GARCH process for the returns, the SSR realized measure, and GK volatility (see, for example, Conrad and Karanasos, 2010). If all twelve Arch and Garman parameters are zero, then we have the AP version of the benchmark HEAVY specification where the only unconditional regressor is the first lag of the powered RM_t. Finally, we should mention that all the parameters in this trivariate system should take non-negative values (see, for example, Conrad and Karanasos, 2010).

To sum up, the bivariate benchmark model (eq. (2)) of Shephard and Sheppard (2010)[3] is characterized by two conditional variance equations, the GARCH(1,0)-X formulation for returns and the GARCH(1,1) formulation for the SSR realized measure:

$$\text{HEAVY-}r\text{: } (1-\beta_r L)\sigma_{rt}^2 = \omega_r + \alpha_{rR} L(RM_t),$$
$$\text{HEAVY-}R\text{: } (1-\beta_R L)\sigma_{Rt}^2 = \omega_R + \alpha_{RR} L(RM_t).$$

Eq. (3) gives the general formulation of our asymmetric power extension, which adds asymmetries, power transformations, and the GK volatility to the benchmark specification. We also use the existing Gaussian quasi-maximum likelihood estimators (QMLE) and multistep-ahead predictors already applied in the APARCH framework (see, for example, He and Teräsvirta, 1999, Laurent, 2004, Karanasos and Kim, 2006). We will first estimate the three conditional variance equations in the general form with all Heavy, Arch, Garman, and Asymmetry parameters given by eq. (3) and in case a parameter is insignificant, we will exclude it and this will result in a reduced form that is statistically preferred for each volatility process. Before the empirical illustration of the proposed model on stock index volatility, we first derive the time series properties of the multivariate AP-HEAVY system and examine its finite-sample performance through a simulation experiment.

3 Theoretical Properties of the Multivariate AP-HEAVY model

3.1 Notation

Throughout this Section, we adhere to the following conventions:

Notation 1 *($\mathbb{Z}_{>0}$) $\mathbb{Z}$, and $\mathbb{Z}_{\geq 0}$ stand for the sets of (positive) integers, and non-negative integers respectively. Similarly, ($\mathbb{R}_{>0}$) $\mathbb{R}$ and $\mathbb{R}_{\geq 0}$ stands for the set of (positive) real numbers, and non-negative real numbers respectively.*

[3] The benchmark HEAVY specification as established by Shephard and Sheppard (2010) does not incorporate our third variable, that is GK volatility.

Notation 2 *We will use upper (lower) case boldface symbols to refer to square matrices (vectors). That is,* $\mathbf{y} = [y_i]_{i=1,\ldots,N}$ *is an* $N \times 1$ *column vector,* $\mathbf{Y} = [y_{ij}]_{i,j=1,\ldots,N}$ *is a square matrix of order* N*.*
$\mathbf{I}_N$ *is the* N*-dimensional identity matrix (hereafter, we will drop the subscript for notational simplicity).*

Notation 3 *Using standard notation,* $\mathbf{Y}'$ *and* $\mathbf{Y}^{-1}$ *are the transpose and the inverse of the square matrix* $\mathbf{Y}$*.* $\mathbf{Y}^{\wedge k} = [y_{ij}^k]$ *is the element-wise exponentiation, whereas* $\mathbf{y}^{\wedge \mathbf{x}} = [y_i^{x_i}]$*, that is the element occupying the* i*-th entry of vector* $\mathbf{y}$ *is raised to the power of the element occupying the* i*-th entry of vector* $\mathbf{x}$*.* $\mathbf{Y}^k = \prod_{i=1}^{k} \mathbf{Y}$ *means that the matrix* $\mathbf{Y}$ *is raised to the power of* k*.*
In addition, $diag[\mathbf{y}]$*, and* $diag[\mathbf{Y}]$ *denote diagonal matrices with elements* y_i *and* y_{ii}*, respectively.*
We will refer to the element-wise absolute value of $\mathbf{Y}$ *as* $|\mathbf{Y}| = [|y_{ij}|]$*. Finally, the inequality* $\mathbf{Y} \geq \mathbf{0}$ *means that all elements of* $\mathbf{Y}$ *are non-negative real numbers.*

Notation 4 *The elementwise expectation operator is denoted by* $\mathbb{E}$*, i.e.,* $\mathbb{E}(\mathbf{Y}) = [\mathbb{E}(y_{ij})]$ *(similarly,* $\mathbb{E}(\mathbf{Y}\,|\mathcal{F}_{t-1}\,)$ *denotes the elementwise, conditional on time* $t-1$*, expectation operator).*

Notation 5 *Let* $\mathbf{Y}^{\otimes 2} = \mathbf{Y} \otimes \mathbf{Y}$*, where* $\otimes$ *is the Kronecker product of two matrices, and* $vec(\mathbf{Y})$ *is a vector in which the columns of the matrix* $\mathbf{Y}$ *are stacked one underneath the other.*

3.2 Multivariate System

In this Section, we will examine the theoretical properties of the multivariate AP-HEAVY model. We will consider the N-dimensional vector process, $\mathbf{r}_t = [r_{it}]$, $i = 1, \ldots, N$, $N \in \mathbb{Z}_{\geq 1}$, $t \in \mathbb{Z}$. For example, for the trivariate case, $r_{1t} = r_t$, $r_{2t} = \widetilde{RM}_t$, and $r_{3t} = \widetilde{GK}_t$. Similarly to eq. (1), we assume that the vector $\mathbf{r}_t$ is characterized by the relation

$$\mathbf{r}_t = \mathbf{Z}_t \boldsymbol{\sigma}_t, \tag{4}$$

where $\mathbf{Z}_t = diag[\mathbf{e}_t]$, $\mathbf{e}_t = [e_{it}]$, and $\boldsymbol{\sigma}_t = [\sigma_{it}]$ is $\mathcal{F}_{t-1}$ measurable with $\mathcal{F}_{t-1} = \sigma(\mathbf{r}_{t-1}, \mathbf{r}_{t-2}, \ldots)$ with $\boldsymbol{\sigma}_t > \mathbf{0}$ for all t. That is, $\mathbf{r}_t = [e_{it}\sigma_{it}]$. Analogously with the assumptions in Section 2.1 the stochastic vector $\mathbf{e}_t = [e_{it}]$ is independent and identically distributed $(i.i.d)$ with $\mathbb{E}(|e_{it}|^{\delta_i}\,|e_{jt}|^{\delta_j}) \in \mathbb{R}_{>0}$ for $i, j = 1, \ldots, N$.

In the N-dimensional (constant conditional correlation) multivariate GARCH model $\mathbf{e}_t$ has zero mean, unit variance, and positive definite time invariant conditional correlation matrix $\mathbf{R} = [\rho_{ij}]$ with $\rho_{ii} = 1$. The conditional covariance matrix of $\mathbf{r}_t$ is denoted by $\mathbf{H}_t = \mathbb{E}(\mathbf{r}_t\mathbf{r}_t'\,|\mathcal{F}_{t-1}\,)$, and it is given by $\mathbf{H}_t = \boldsymbol{\Sigma}_t\mathbf{R}\boldsymbol{\Sigma}_t$, where $\boldsymbol{\Sigma}_t = diag[\boldsymbol{\sigma}_t] = diag[\mathbf{H}_t^{\frac{1}{2}}]$.

The N-dimensional AP-HEAVY$(1,1)$ model is given by

$$(\mathbf{I} - \mathbf{B}L)\boldsymbol{\sigma}_t^{\wedge \boldsymbol{\delta}} = \boldsymbol{\omega} + L\mathbf{A}_t\,|\mathbf{r}_t|^{\wedge \boldsymbol{\delta}}\,, \tag{5}$$

where $\boldsymbol{\delta} = [\delta_i]$, is the vector with the power parameters with $\delta_i \in \mathbb{R}_{>0}$ for all i, $\boldsymbol{\sigma}_t^{\wedge\boldsymbol{\delta}} = [\sigma_{it}^{\delta_i}]$, and $|\mathbf{r}_t|^{\wedge\boldsymbol{\delta}} = [|e_{it}|^{\delta_i}\, \sigma_{it}^{\delta_i}]$ (we recall that $\mathbf{r}_t$ and $\boldsymbol{\sigma}_t$ have been defined in eq. (4)). $\mathbf{B} = [\beta_{ii}]$ is a diagonal matrix (of order N); $\boldsymbol{\omega} = [\omega_i]$ is a vector that contains the drifts; $\mathbf{A}_t = \mathbf{A} + \boldsymbol{\Gamma}_t$, where $\mathbf{A} = [\alpha_{ij}]$ and $\boldsymbol{\Gamma}_t = [\boldsymbol{\gamma}_{ij} s_{jt}]$, are N-dimensional full matrices. Note that $\boldsymbol{\Gamma}_t$ can be written as $\boldsymbol{\Gamma}_t = \boldsymbol{\Gamma} diag[\mathbf{s}_t]$ where $\boldsymbol{\Gamma} = [\gamma_{ij}]$ and $\mathbf{s}_t = [s_{it}]$. The cross diagonal elements of $\mathbf{A}$ capture the shock (or unconditional) spillovers, whereas those of $\boldsymbol{\Gamma}_t$ capture the asymmetric shock spillovers.

3.2.1 Weak VARMA Representation

In order to derive the optimal predictors, we need to obtain the weak VARMA representation of the model in eq. (5). First, we will introduce the following definitions.

Definition 1 *i) Let* $\mathbf{Z}(\boldsymbol{\delta}) = \mathbb{E}(|\mathbf{Z_t}|^{\wedge\boldsymbol{\delta}})$ *be a diagonal matrix with the element occupying the i-th entry denoted by* $z_i = \mathbb{E}(|e_{it}|^{\delta_i})$,
ii) Define the serially uncorrelated vector with, under (see below) Condition 1, zero mean as follows: $\mathbf{v}_t(\boldsymbol{\delta}) = |\mathbf{r}_t|^{\wedge\boldsymbol{\delta}} - \mathbb{E}(|\mathbf{r}_t|^{\wedge\boldsymbol{\delta}}\,|\mathcal{F}_{t-1})$. *In view of eq. (4),* $\mathbf{v}_t$ *can be written as*

$$\mathbf{v}_t = |\mathbf{r}_t|^{\wedge\boldsymbol{\delta}} - \mathbf{Z}\boldsymbol{\sigma}_t^{\wedge\boldsymbol{\delta}} = \left(|\mathbf{Z}_t|^{\wedge\boldsymbol{\delta}} - \mathbf{Z}\right)\boldsymbol{\sigma}_t^{\wedge\boldsymbol{\delta}}$$

(to lighten the notation, in what follows we drop the parenthesis $\boldsymbol{\delta}$; we recall that $\boldsymbol{\delta}$ is given in eq. (5).

Proposition 1 *The weak VARMA(1,1) representation of the N-dimensional AP-HEAVY* $(1,1)$ *process is given by*

$$[\mathbf{I} - L\mathbf{C}_t]\boldsymbol{\sigma}_t^{\wedge\boldsymbol{\delta}} = \boldsymbol{\omega} + L\mathbf{A}_t\mathbf{v}_t, \tag{6}$$

where

$$\mathbf{C}_t = \mathbf{B} + \mathbf{A}_t\mathbf{Z}$$

($\mathbf{B}$ and $\mathbf{A}_t$ have been defined in eq. (5); notice that $\mathbf{C}_t$ depends on $\boldsymbol{\delta}$, but again in order to simplify the notation we will use $\mathbf{C}_t$ instead of $\mathbf{C}_t(\boldsymbol{\delta})$).

The proof is trivial: we add and subtract $\mathbf{A}_{t-1}\mathbf{Z}\boldsymbol{\sigma}_{t-1}^{\wedge\boldsymbol{\delta}}$ in the right-hand side of eq. (5).

Next, let us call

$$\mathbf{D}_{t,k} = \prod_{r=0}^{k-1} \mathbf{C}_{t-1-r}, \tag{7}$$

where $k \in \mathbb{Z}_{\geq 1}$. We further extend the definition of $\mathbf{D}_{t,k}$ by assigning the initial matrix value $\mathbf{D}_{t,0} = \mathbf{I}_N$.

3.2.2 General Solution

Next, we will present the general solution, which generates all the main time series properties of the AP-HEAVY multivariate system.

Theorem 1 *The general solution of the weak VARMA representation in eq. (6) under the initial matrix value* $\boldsymbol{\sigma}_{t-k}^{\wedge\boldsymbol{\delta}}$*, is given by*

$$\boldsymbol{\sigma}_t^{\wedge\boldsymbol{\delta}} = \underbrace{\sum_{r=1}^{k} \mathbf{D}_{t,r-1}\left(\boldsymbol{\omega} + \mathbf{A}_{t-r}\mathbf{v}_{t-r}\right)}_{(Particular\ Solution)} + \underbrace{\mathbf{D}_{t,k}\boldsymbol{\sigma}_{t-k}^{\wedge\boldsymbol{\delta}}}_{(Homogeneous\ Sol.)} . \tag{8}$$

The proof is trivial. It is obtained by using repeated substitution in eq. (6).

In the above Proposition $\boldsymbol{\sigma}_t^{\wedge\boldsymbol{\delta}}$ is decomposed into two parts. The homogeneous solution, which consists of the initial (matrix) value $\boldsymbol{\sigma}_{t-k}^{\wedge\boldsymbol{\delta}}$ times $\mathbf{D}_{t,k}$, and the particular one that is formed by products involving the matrix $\mathbf{D}_{t,r-1}$ times i) the drift $\boldsymbol{\omega}$, and ii) the matrix $\mathbf{A}_{t-r}$ times the serially uncorrelated vector $\mathbf{v}_{t-r}$.

Remark 1 *When* $k = 1$ *the general solution in Theorem 1 coincides with eq. (6). This is a consequence of the following statement:* $\mathbf{D}_{t,0} = \mathbf{I}$ *and* $\mathbf{D}_{t,1} = \mathbf{C}_{t-1}$ *(see eq. (7)).*

3.2.3 Optimal Predictors

In what follows, we will obtain the linear predictor of the AP-HEAVY system.

First, we will introduce some additional notation.

Notation 6 *i) Let the expected value of* $\mathbf{C}_t$ *and* $\mathbf{A}_t$ *be denoted as* $\mathbf{C} = \mathbb{E}(\mathbf{C}_t)$ *and* $\overline{\mathbf{A}} = \mathbb{E}(\mathbf{A}_t)$ *respectively (where* $\mathbf{C}_t$ *is given in eq. (6)). Thus*

$$\mathbf{C} = \mathbf{B} + \overline{\mathbf{A}}\mathbf{Z}, \ \textit{with}\ \overline{\mathbf{A}} = \left(\mathbf{A} + \boldsymbol{\Gamma}\frac{\mathbf{1}}{\mathbf{2}}\right) \tag{9}$$

(since $\mathbb{E}[diag[\mathbf{s}_t]] = \mathbb{E}[diag[\mathbf{s}_t^2]] = (1/2)\mathbf{I}$*), and thus eq. (7) implies that* $\mathbb{E}(\mathbf{D}_{t,k}) = \mathbf{C}^k$*.*

ii) Let $\rho_{\max}(\mathbf{C})$ *refer to the modulus of the largest eigenvalue of* $\mathbf{C}$*.*

iii) Let $(\Omega, \digamma, P)$ *be a probability space and* $L_2(\Omega, \digamma, P)$ *(in short* L_2*) be the Hilbert space of random variables with finite first and second moments defined on* $(\Omega, \digamma, P)$*.*

Condition 1 $\rho_{\max}(\mathbf{C}) < 1$.

Taking the conditional expectation of eq. (8) with respect to the σ field $\mathcal{F}_{t-k-1}$ yields the following Proposition.

Proposition 2 *The k-step-ahead optimal (in L_2 sense) linear predictor of the powered transformed $\boldsymbol{\sigma}_t$ for the N-dimensional AP-HEAVY(1, 1) model is readily seen to be*

$$\mathbb{E}(\boldsymbol{\sigma}_t^{\wedge\boldsymbol{\delta}} \,|\mathcal{F}_{t-k-1}) = (\mathbf{I}-\mathbf{C})^{-1}(\mathbf{I}-\mathbf{C}^k)\boldsymbol{\omega} + \mathbf{C}^k\boldsymbol{\sigma}_{t-k}^{\wedge\boldsymbol{\delta}}. \tag{10}$$

Under Condition 1 the unconditional mean of $\boldsymbol{\sigma}_t^{\wedge\boldsymbol{\delta}}$, that is $\boldsymbol{\sigma}(\boldsymbol{\delta}) = \mathbb{E}(\boldsymbol{\sigma}_t^{\wedge\boldsymbol{\delta}})$ is equal to the $\lim_{k\to\infty}\mathbb{E}(\boldsymbol{\sigma}_t^{\wedge\boldsymbol{\delta}}\,|\mathcal{F}_{t-k-1})$, and thus it is given by

$$\boldsymbol{\sigma} = (\mathbf{I}-\mathbf{C})^{-1}\boldsymbol{\omega}. \tag{11}$$

(where $\mathbf{C}$ has been defined in eq. (9)).

Finally, the following Proposition gives the optimal linear predictor of the power transformed observed vector $|\mathbf{r}_t|^{\wedge\boldsymbol{\delta}}$ as well as its first unconditional moment.

Proposition 3 *The k-step-ahead optimal (in L_2 sense) linear predictor of $|\mathbf{r}_t|^{\wedge\boldsymbol{\delta}}$ is given by*

$$\mathbb{E}(|\mathbf{r}_t|^{\wedge\boldsymbol{\delta}}\,|\mathcal{F}_{t-k-1}) = \mathbf{Z}\mathbb{E}(\boldsymbol{\sigma}_t^{\wedge\boldsymbol{\delta}}\,|\mathcal{F}_{t-k-1}),$$

($\mathbf{Z}$ has been defined in Definition 1(i), and eq. (10) gives $\mathbb{E}(\boldsymbol{\sigma}_t^{\wedge\boldsymbol{\delta}}\,|\mathcal{F}_{t-k-1})$).
Under Condition 1, the unconditional mean of $|\mathbf{r}_t|^{\wedge\boldsymbol{\delta}}$, that is $\mathbf{r}(\boldsymbol{\delta}) = \mathbb{E}(|\mathbf{r}_t|^{\wedge\boldsymbol{\delta}})$ is equal to $\lim_{k\to\infty}\mathbb{E}(|\mathbf{r}_t|^{\wedge\boldsymbol{\delta}}\,|\mathcal{F}_{t-k-1})$, and thus it is given by

$$\mathbf{r} = \mathbf{Z}\boldsymbol{\sigma}. \tag{12}$$

The proof is trivial. It follows from the definition of $|\mathbf{r}_t|^{\wedge\boldsymbol{\delta}}$ in eq. (4) and Proposition 2. Alternatively, we could obtain the optimal linear predictor and the first unconditional moment of $|\mathbf{r}_t|^{\wedge\boldsymbol{\delta}}$ using its weak VARMA(1, 1) representation, which is not difficult to show (proof is not reported but it is available upon request) that it is given by:

$$[\mathbf{I}-L\mathbf{C}_t]\,|\mathbf{r}_t|^{\wedge\boldsymbol{\delta}} = \mathbf{Z}\boldsymbol{\omega} + (\mathbf{I}-\mathbf{B}L)\mathbf{v}_t.$$

A Comparison

Next, we provide a comparison between the benchmark HEAVY system and the more general AP specification. Their difference is captured by the matrix $\mathbf{C}$ (see eq. (9)). We will examine the bivariate case, which is when $N = 2$. For the more general double asymmetric power (DAP) specification, $\mathbf{C}$ is a full matrix with: i) diagonal elements given by $\beta_i + (\alpha_{ii} + \gamma_{ii}/2)z_i$, $i = r, R$, we recall that $z_i = \mathbb{E}(|e_{it}|^{\delta_i})$, and ii) off-diagonal elements given by $(\alpha_{ij} + \gamma_{ij})z_j$, $i, j = r, R$, for $i \neq j$. For the benchmark model, since $\gamma_{ij} = 0$, $z_i = 1$, for all $i, j = r, R$, and $\alpha_{Ri} = 0$, $\mathbf{C}$ is restricted to being an upper diagonal matrix. That

is, we have

$$\text{DAP Specification: } \mathbf{C}= \begin{bmatrix} \beta_r + (\alpha_{rr} + \gamma_{rr}/2)z_r & (\alpha_{rR} + \gamma_{rR}/2)z_R \\ (\alpha_{Rr} + \gamma_{Rr}/2)z_r & \beta_R + (\alpha_{RR} + \gamma_{RR}/2)z_R \end{bmatrix}$$

$$\text{Benchmark HEAVY: } \mathbf{C}= \begin{bmatrix} \beta_r & \alpha_{rR} \\ 0 & \beta_R + \alpha_{RR} \end{bmatrix}.$$

Figure 1 presents the comparison of the benchmark and DAP-HEAVY models' forecasting performance (see also Section 5). We apply the optimal predictor of $|\mathbf{r}_t|^{\wedge \boldsymbol{\delta}}$ (under Proposition 3) on Dow Jones returns and realized variance data and calculate 50-step-ahead forecasts. The more general specification produces forecasts significantly closer to the actual values for both returns (Fig.1, a & b) and realized measure (Fig.1, c & d). Most importantly, its forecasts are more accurate in peaks of returns and realized variance actual values. The benchmark model remains behind our proposed asymmetric power extension in predicting low- and high-frequency volatility indicators. It produces, mostly, lower volatility forecasts (dotted lines) in comparison with the DAP (dashed lines) and actual (solid lines) values. Therefore, our first contribution, which is the asymmetric power extension, provides a significant improvement on the HEAVY system of Shephard and Sheppard (2010).

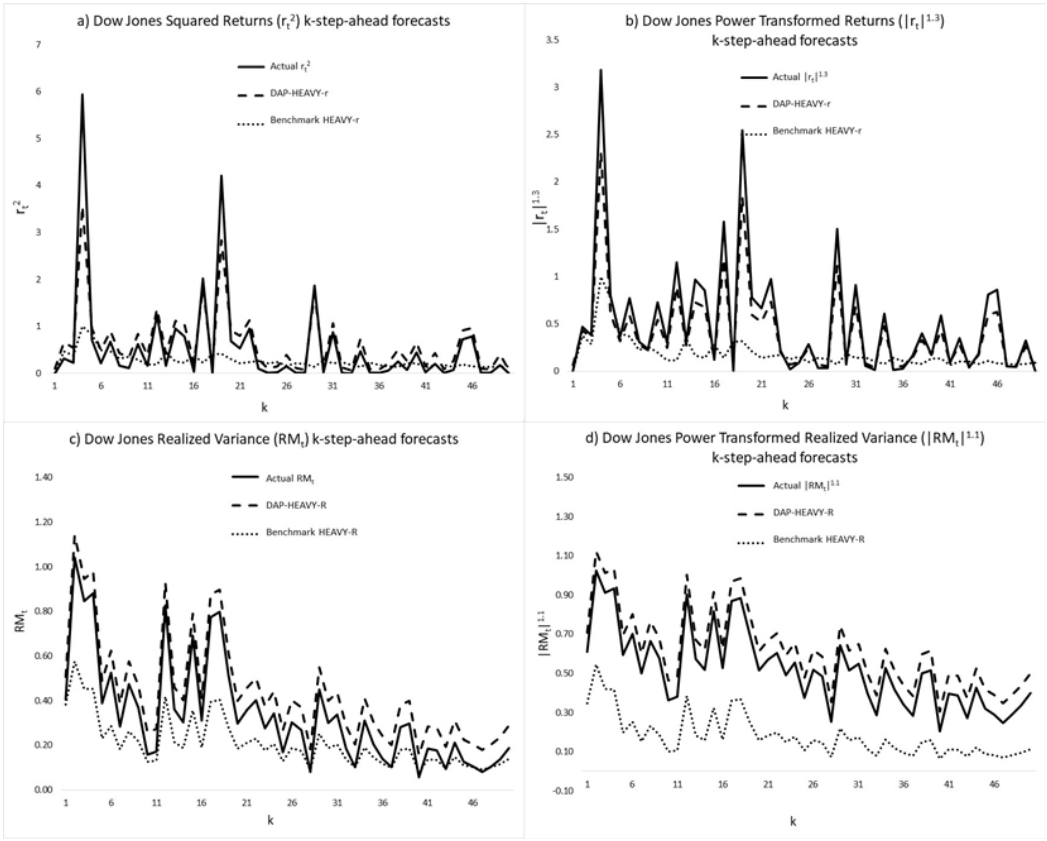

Figure 1. Dow Jones Returns and Realized Variance k-step-ahead forecasts

3.3 Second Moments

Now that we have derived the optimal predictors and the first unconditional moment of the AP-HEAVY system, we will examine its second moment structure.

3.3.1 Notation

But first, we will introduce some further notation.

Covariances

Let $\mathbf{\Gamma}(\ell;\boldsymbol{\delta}) = [\gamma_{ij}(\ell;\boldsymbol{\delta})]$, $\ell \in \mathbb{Z}_{\geq 0}$, be the multidimensional covariance function of $\{\boldsymbol{\sigma}_t^{\wedge\boldsymbol{\delta}}\}$; as usual in what follows we will suppress the index $\boldsymbol{\delta}$ for ease of notation, that is we will use $\mathbf{\Gamma}(\ell;\boldsymbol{\delta}) = \mathbf{\Gamma}(\ell)$. In view of this definition we have:

$$\mathbf{\Gamma}(\ell) = \mathbb{E}[(\boldsymbol{\sigma}_{t-\ell}^{\wedge\boldsymbol{\delta}} - \boldsymbol{\sigma})(\boldsymbol{\sigma}_t^{\wedge\boldsymbol{\delta}} - \boldsymbol{\sigma})'] = \mathbf{\Sigma}(\ell) - \boldsymbol{\sigma}\boldsymbol{\sigma}', \tag{13}$$

where $\mathbf{\Sigma}(\ell) = \mathbb{E}(\boldsymbol{\sigma}_{t-\ell}^{\wedge\boldsymbol{\delta}}(\boldsymbol{\sigma}_t^{\wedge\boldsymbol{\delta}})')$. In addition, let the vectorizations of $\mathbf{\Sigma}(\ell)$ and $\mathbf{\Gamma}(\ell)$ be denoted by $\mathbf{s}(\ell)$ and $\boldsymbol{\gamma}(\ell)$, respectively. Explicit solutions for the $\mathbf{\Gamma}(\ell)$ and conditions for its existence will be presented below.

Further, let

$$\mathbf{D} = diag[\sqrt{\gamma_{11}(0)}, \ldots, \sqrt{\gamma_{NN}(0)}],$$

where $\gamma_{ii}(0)$ is the element occupying the i-th diagonal entry of $\mathbf{\Gamma}(0)$. To further fix notation, write the ℓ-th order, for $\ell \geq 1$, autocorrelation matrix of $\boldsymbol{\sigma}_t^{\wedge\boldsymbol{\delta}}$ as

$$\mathbf{R}(\ell) = \mathbf{D}^{-1}\mathbf{\Gamma}(\ell)\mathbf{D}^{-1}.$$

Kronecker Products

In what follows we will introduce some additional notation, which involves various Kronecker products.

Notation 7 *Let*

$$\mathbf{C}^{\otimes 2} = \mathbf{C} \otimes \mathbf{C}, \quad \overline{\mathbf{A}}^{\otimes 2} = \overline{\mathbf{A}} \otimes \overline{\mathbf{A}}, \tag{14}$$

where $\mathbf{C}$ *and* $\overline{\mathbf{A}}$ *have been defined in eq. (9).*

We continue by introducing the following notation.

Notation 8 *Let*

$$\mathbf{Z}^{\otimes 2} = \mathbf{Z} \otimes \mathbf{Z}, \; \mathbb{E}\left[\left(|\mathbf{Z}_t|^{\wedge\boldsymbol{\delta}}\right)^{\otimes 2}\right] = \mathbb{E}(|\mathbf{Z}_t|^{\wedge\boldsymbol{\delta}} \otimes |\mathbf{Z}_t|^{\wedge\boldsymbol{\delta}}),$$
$$\widetilde{\mathbf{Z}} = \left[\mathbb{E}\left(|\mathbf{Z}_t|^{\wedge\boldsymbol{\delta}}\right)^{\otimes 2}\right] - \mathbf{Z}^{\otimes 2} = \mathbb{E}\left[\left(|\mathbf{Z}_t|^{\wedge\boldsymbol{\delta}} - \mathbf{Z}\right)^{\otimes 2}\right],$$

be three diagonal matrices of order N^2 *(*$\mathbf{Z}_t$ *and* $\mathbf{Z}$ *have been defined in eq. (4) and Definition 1(i), respectively).*

Remark 2 *The element occupying the* r*-th diagonal entry of* $\widetilde{\mathbf{Z}}$*, with* $r = [(i-1)N + j]$*, where* $i, j = 1, \ldots, N$*, is given by*

$$\mathbb{E}(|e_{it}|^{\delta_i}\,|e_{jt}|^{\delta_j}) - \mathbb{E}(\left|e_{(it}\right|^{\delta_i})\mathbb{E}(|e_{jt}|^{\delta_j}).$$

Notation 9 *Let*

$$\widetilde{\mathbf{C}} = \mathbf{C}^{\otimes 2} + \overline{\mathbf{A}}^{\otimes 2}\widetilde{\mathbf{Z}} \tag{15}$$

(where $\mathbf{C}^{\otimes 2}$ *and* $\overline{\mathbf{A}}^{\otimes 2}$ *are given in eq. (14), and* $\widetilde{\mathbf{Z}}$ *is defined in Notation 8.*

Condition 2 $\rho_{\max}(\widetilde{\mathbf{C}}) < 1$.

3.3.2 Covariance Structure

In the following theorem, we will present an explicit formula for $\boldsymbol{\gamma}(0)$.

Theorem 2 *Consider the N-dimensional vector AP-HEAVY $(1,1)$ process. Under Condition 2 the vectorization of $\boldsymbol{\Gamma}(0)$, is given by*

$$\boldsymbol{\gamma}(0) = \left(\mathbf{I}_{N^2} - \widetilde{\mathbf{C}}\right)^{-1} \overline{\mathbf{A}}^{\otimes 2} \widetilde{\mathbf{Z}} \boldsymbol{\sigma}^{\otimes 2}. \tag{16}$$

Further, $\boldsymbol{\gamma}(\ell)$, for $\ell \geq 1$, is given by

$$\boldsymbol{\gamma}(\ell) = \left(\mathbf{C}^{\ell} \otimes \mathbf{I}\right) \boldsymbol{\gamma}(0). \tag{17}$$

Next, let us denote the multidimensional covariance function of $\{|\mathbf{r}_t|^{\wedge \boldsymbol{\delta}}\}$ by $\boldsymbol{\Gamma}_r(\ell) = [\gamma_{ij,r}(\ell)]$.

Theorem 3 *Consider the N-dimensional vector AP-HEAVY $(1,1)$ process. Under Condition 2 the vectorization of $\boldsymbol{\Gamma}_r(0)$, is given by*

$$\boldsymbol{\gamma}_r(0) = \left[\mathbb{E}\left[\left(|\mathbf{Z}_t|^{\wedge \boldsymbol{\delta}}\right)^{\otimes 2}\right]\left(\mathbf{I}_{N^2} - \widetilde{\mathbf{C}}\right)^{-1} \overline{\mathbf{A}}^{\otimes 2} + \mathbf{I}_{N^2}\right] \widetilde{\mathbf{Z}} \boldsymbol{\sigma}^{\otimes 2} \tag{18}$$

Moreover, $\boldsymbol{\gamma}_r(\ell)$, for $\ell \geq 1$, is given by

$$\boldsymbol{\gamma}_r(\ell) = \mathbf{Z} \boldsymbol{\gamma}_r(0). \tag{19}$$

In Appendix A, we derive the proofs of Theorems 2 and 3.

3.4 Simulations

After deriving the time series properties of the multivariate AP-HEAVY system, we examine the finite-sample performance of the diagnostic tests employed in terms of both their size and power properties. Given that simulation studies have already widely explored the finite-sample properties of the univariate (AP-)GARCH-X and the multivariate GARCH with volatility spillovers ($\mathbf{A}$ and $\mathbf{B}$ full matrices) but without asymmetries, that is the $\boldsymbol{\Gamma}$ full matrix, (see, for example, Lundbergh and Teräsvirta, 2002, Halunga and Orme, 2009, Francq and Thieu, 2019, Pedersen and Rahbek, 2019, Li et al., 2019, Nakatani and Teräsvirta, 2009, Pedersen, 2017), here in the multivariate AP-HEAVY/GARCH case, we choose to focus our simulation experiment on the significance of the asymmetric effects, the Sign Bias Test (SBT) of Engle and Ng (1993) accounting for both own and cross leverage of each equation in the system, and the likelihood-ratio test (LRT) for model selection (benchmark vs AP-HEAVY). We conduct the Monte Carlo simulations in OxMetrics 7 for the bivariate case of the Asymmetric Power specification with own and cross Arch and Heavy parameters. For each data-generating process (DGP) with Gaussian innovations drawn from the standard Normal distribution (e_{1t}, e_{2t} ˜ $IIDN(0,1)$), we use the sample sizes

$T = 1000$, 2500, 5000, $10,000$ after discarding the first 1000 observations to avoid initialization effects. All simulations are based on 5000 replications and the empirical rejection frequencies are compared with the 5% nominal size of each test.

We first consider the size properties of the SBT statistic for the DGPs 1-5 reported in Table 1, Panel A. We test five different specifications of the bivariate benchmark Heavy. The SBT statistic is calculated on each equation (e_{1t} and e_{2t} processes) with similar results and the actual rejection frequencies from both equations are stated in Table 2, Panel A. The SBT results suggest that significant sign effects are omitted by the benchmark specification. For DGPs 3 and 5, the test is relatively undersized in the sample size $T = 1000$ and slightly oversized in the sample size $T = 10,000$. Overall, our Monte Carlo experiment shows that in most cases the sign bias test has reasonable size properties quite close to the 5% nominal level in larger samples.

Next, the simulations for the power of the sign bias test are based on DGPs 6-10 (Table 1, Panel B) corresponding to five bivariate AP-HEAVY models. The $\mathbf{B}$ matrix remains diagonal as in the benchmark case, that is without volatility spillovers from the cross Garch effects ($\beta_{12} = \beta_{21} = 0$). The $\mathbf{A}$ matrix is either a full matrix with all own and cross Arch effects (DGPs 9 & 10) or with the own Arch effect excluded in the first equation (DGPs 6-8), similarly to the returns and the Garman Klass volatility equations estimated in our empirical application (see Tables 5A and 5C below). The $\mathbf{\Gamma}$ matrix contains the leverage parameters, either own asymmetries (OAP model, DGP 6) or cross asymmetries (CAP model, DGP 7) or a full matrix with both own and cross asymmetric effects (DAP model, DGPs 8-10). The power transformations in $\boldsymbol{\delta}$ are common for both equations in the system with $\delta_i = 1.5$ for DGPs 6-9. In the case of DGP 10, we test different powers ($\delta_1 = 1.5$ and $\delta_2 = 1.0$) for the conditional variance of the two processes. Table 2, Panel B reports the SBT power simulation results with significant asymmetric effects not ignored across all AP-HEAVY models considered. The power of the test improves as the sample size increases for most DGPs, while in the DAP models with full $\mathbf{\Gamma}$ matrix (DGPs 8-10) the power is already high from smaller samples.

Finally, we perform the likelihood ratio test of the AP model compared with the benchmark one for both equations. We consider DGPs 6-10 as the unrestricted specifications and the corresponding benchmark ones (with $\mathbf{\Gamma} = \mathbf{0}$ and $\alpha_{11} = \alpha_{21} = 0$) as the restricted cases. The LRT results in Table 2, Panel C support the superiority of the asymmetric models to the benchmark formulations. The test suggests the significant improvement in terms of the log-likelihood maximization for the more richly parametrized unrestricted models versus the respective restricted cases.

All in all, the simulation experiment suggests very good size and power properties of the SBT in detecting asymmetries in the HEAVY framework and quite good performance of the LRT for model selection across all sample sizes. Furthermore, our simulation results have also shown that the empirical

distribution of the t-statistics of all estimated parameters in both equations is quite close to normal (the average difference of the true parameter and its estimate [bias], the standard error and the root mean square error of the estimate are available upon request for all parameters), mostly converging to normal in higher sample sizes regardless of the degree of persistence tested under each DGP, and at the same time validating the finite-sample performance of the QML estimators. In the remaining part of the paper, the AP-HEAVY model's overperformance in- and out-of-sample is further illustrated through an empirical application on stock index data (Sections 4 and 5).

Table 1. DGPs for size & power simulations

Heavy models	DGPs	$\mathbf{A}$	$\mathbf{B}$	$\mathbf{\Gamma}$	$\boldsymbol{\delta}$
Panel A: Size simulations					
Benchmark	DGP 1	$\begin{bmatrix} 0 & 0.30 \\ 0 & 0.40 \end{bmatrix}$	$\begin{bmatrix} 0.65 & 0 \\ 0 & 0.55 \end{bmatrix}$	$\begin{bmatrix} 0 & 0 \\ 0 & 0 \end{bmatrix}$	$\begin{bmatrix} 2.0 \\ 2.0 \end{bmatrix}$
Benchmark	DGP 2	$\begin{bmatrix} 0 & 0.20 \\ 0 & 0.40 \end{bmatrix}$	$\begin{bmatrix} 0.75 & 0 \\ 0 & 0.60 \end{bmatrix}$	$\begin{bmatrix} 0 & 0 \\ 0 & 0 \end{bmatrix}$	$\begin{bmatrix} 2.0 \\ 2.0 \end{bmatrix}$
Benchmark	DGP 3	$\begin{bmatrix} 0 & 0.25 \\ 0 & 0.35 \end{bmatrix}$	$\begin{bmatrix} 0.85 & 0 \\ 0 & 0.65 \end{bmatrix}$	$\begin{bmatrix} 0 & 0 \\ 0 & 0 \end{bmatrix}$	$\begin{bmatrix} 2.0 \\ 2.0 \end{bmatrix}$
Benchmark	DGP 4	$\begin{bmatrix} 0 & 0.18 \\ 0 & 0.25 \end{bmatrix}$	$\begin{bmatrix} 0.80 & 0 \\ 0 & 0.70 \end{bmatrix}$	$\begin{bmatrix} 0 & 0 \\ 0 & 0 \end{bmatrix}$	$\begin{bmatrix} 2.0 \\ 2.0 \end{bmatrix}$
Benchmark	DGP 5	$\begin{bmatrix} 0 & 0.30 \\ 0 & 0.30 \end{bmatrix}$	$\begin{bmatrix} 0.80 & 0 \\ 0 & 0.70 \end{bmatrix}$	$\begin{bmatrix} 0 & 0 \\ 0 & 0 \end{bmatrix}$	$\begin{bmatrix} 2.0 \\ 2.0 \end{bmatrix}$
Panel B: Power simulations					
OAP	DGP 6	$\begin{bmatrix} 0 & 0.10 \\ 0.05 & 0.10 \end{bmatrix}$	$\begin{bmatrix} 0.80 & 0 \\ 0 & 0.70 \end{bmatrix}$	$\begin{bmatrix} 0.08 & 0 \\ 0 & 0.10 \end{bmatrix}$	$\begin{bmatrix} 1.5 \\ 1.5 \end{bmatrix}$
CAP	DGP 7	$\begin{bmatrix} 0 & 0.10 \\ 0.05 & 0.10 \end{bmatrix}$	$\begin{bmatrix} 0.80 & 0 \\ 0 & 0.70 \end{bmatrix}$	$\begin{bmatrix} 0 & 0.08 \\ 0.10 & 0 \end{bmatrix}$	$\begin{bmatrix} 1.5 \\ 1.5 \end{bmatrix}$
DAP	DGP 8	$\begin{bmatrix} 0 & 0.10 \\ 0.05 & 0.10 \end{bmatrix}$	$\begin{bmatrix} 0.80 & 0 \\ 0 & 0.70 \end{bmatrix}$	$\begin{bmatrix} 0.08 & 0.10 \\ 0.05 & 0.10 \end{bmatrix}$	$\begin{bmatrix} 1.5 \\ 1.5 \end{bmatrix}$
DAP	DGP 9	$\begin{bmatrix} 0.04 & 0.10 \\ 0.05 & 0.10 \end{bmatrix}$	$\begin{bmatrix} 0.80 & 0 \\ 0 & 0.70 \end{bmatrix}$	$\begin{bmatrix} 0.05 & 0.05 \\ 0.05 & 0.10 \end{bmatrix}$	$\begin{bmatrix} 1.5 \\ 1.5 \end{bmatrix}$
DAP	DGP 10	$\begin{bmatrix} 0.04 & 0.10 \\ 0.05 & 0.10 \end{bmatrix}$	$\begin{bmatrix} 0.80 & 0 \\ 0 & 0.70 \end{bmatrix}$	$\begin{bmatrix} 0.05 & 0.05 \\ 0.05 & 0.10 \end{bmatrix}$	$\begin{bmatrix} 1.5 \\ 1.0 \end{bmatrix}$

Notes: For all DGPs $\boldsymbol{\omega} = \begin{bmatrix} 0.01 \\ 0.02 \end{bmatrix}$.

Table 2. Size & power simulation results

	1st equation (e_{1t})					2nd equation (e_{2t})				
Panel A: Size simulations (SBT empirical rejection frequencies)										
T	DGP 1	DGP 2	DGP 3	DGP 4	DGP 5	DGP 1	DGP 2	DGP 3	DGP 4	DGP 5
1000	0.031	0.046	0.009	0.059	0.010	0.026	0.039	0.001	0.051	0.012
2500	0.035	0.041	0.030	0.044	0.045	0.031	0.040	0.036	0.040	0.047
5000	0.040	0.049	0.041	0.039	0.049	0.049	0.055	0.049	0.047	0.043
10,000	0.046	0.052	0.058	0.045	0.059	0.046	0.052	0.055	0.048	0.061
Panel B: Power simulations (SBT empirical rejection frequencies)										
T	DGP 6	DGP 7	DGP 8	DGP 9	DGP 10	DGP 6	DGP 7	DGP 8	DGP 9	DGP 10
1000	0.442	0.204	0.632	0.841	0.809	0.506	0.233	0.701	0.892	0.831
2500	0.261	0.356	0.891	0.992	0.878	0.286	0.447	0.856	0.976	0.924
5000	0.755	0.694	0.949	0.997	1.000	0.623	0.688	0.991	0.999	1.000
10,000	0.893	0.905	0.995	1.000	1.000	0.850	0.969	1.000	1.000	1.000
Panel C: LRT p-values for AP (unrestricted) vs benchmark (restricted) Heavy specification										
T	DGP 6	DGP 7	DGP 8	DGP 9	DGP 10	DGP 6	DGP 7	DGP 8	DGP 9	DGP 10
1000	0.043	0.067	0.011	0.014	0.000	0.038	0.044	0.009	0.020	0.010
2500	0.037	0.055	0.025	0.018	0.001	0.042	0.041	0.019	0.027	0.003
5000	0.049	0.048	0.008	0.022	0.031	0.047	0.051	0.012	0.026	0.036
10,000	0.050	0.046	0.030	0.020	0.018	0.052	0.048	0.036	0.018	0.024

Notes: Empirical rejection frequencies based on the 5% nominal level..

4 Empirical Application

4.1 Data Description

We provide an empirical application of the HEAVY framework on five stock indices' returns, realized and GK volatilities. We use daily data for five stock market indices extracted from the Oxford-Man Institute's (OMI) realized library version 0.3 of Heber et al. (2009): Dow Jones Industrial Average from the US (DJ), Korea Composite Stock Price Index from South Korea (KOSPI), CAC 40 from France (CAC), All Ordinaries from Australia (AORD), and MXSE IPC from Mexico (IPC). Our sample covers the period from 03/01/2000 to 30/09/2019 for most indices. The OMI's realized library includes daily stock market returns and several realized volatility measures calculated on high-frequency data from the

Reuters DataScope Tick History database. The data are first cleaned and then used in the realized measures calculations. According to the library's documentation, the data cleaning consists of deleting records outside the time interval that the stock exchange is open. Some minor manual changes are also needed when results are ineligible due to the rebasing of indices. We use the daily closing prices, P_t^C, to form the daily returns as follows: $r_t = \ln(P_t^C) - \ln(P_{t-1}^C)$, and two realized measures as drawn from the library: the realized kernel and the 5-minute realized variance. The estimation results using the two alternative measures are very similar, so we present only the ones with the realized variance (the results for the realized kernel are available upon request).

4.1.1 Realized Measures

The library's realized measures are calculated in the way described in Shephard and Sheppard (2010). The realized kernel, which we use as an alternative to the realized variance (results are not reported but they are available upon request), is calculated using a Parzen weight function as follows: $RK_t = \sum_{k=-H}^{H} k(h/(H+1))\gamma_h$, where $k(x)$ is the Parzen kernel function with $\gamma_h = \sum_{j=|h|+1}^{n} x_{j,t}x_{j-|h|,t}$; $x_{jt} = X_{t_{j,t}} - X_{t_{j-1,t}}$ are the 5-minute intra-daily returns where $X_{t_{j,t}}$ are the intra-daily log-prices and $t_{j,t}$ are the times of trades on the t-th day. Shephard and Sheppard (2010) declared that they selected the bandwidth of H as in Barndorff-Nielsen et al. (2009).

The 5-minute realized variance, RV_t, which we choose to present here, is calculated with the formula: $RV_t = \sum x_{j,t}^2$. Heber et al. (2009) additionally implement a subsampling procedure from the data to the most feasible level in order to eliminate the stock market noise effects. The subsampling involves averaging across many realized variance estimations from different data subsets (see also the references in Shephard and Sheppard, 2010 for realized measures surveys', noise effects, and subsampling procedures).

4.1.2 GK Volatility

Using data on the daily high, low, opening, and closing prices of each index in the OMI's realized library we generate an additional daily measure of price volatility. To avoid the microstructure biases introduced by high-frequency data and based on the conclusion of Chen et al. (2006), that the range-based and high-frequency integrated volatility provide essentially equivalent results, we construct the daily GK volatility as follows:

$$GK_t = \frac{1}{2}u_t^2 - (2\ln 2 - 1)c_t^2,$$

where u_t and c_t are the differences in the natural logarithms (as of time t) of the high and low and of the closing and opening prices, respectively. The Garman-Klass is an open-to-close range-based volatility estimator that is documented as a more precise volatility proxy, with superior empirical performance in

the GARCH framework. Recently, Molnár (2016) has demonstrated that the inclusion of the Parkinson and GK estimators in the Range-GARCH model he proposed, outperforms the standard GARCH$(1,1)$, and it performs particularly better in situations, where volatility level changes rapidly. Several studies have also discussed the improvement of the GARCH framework through the open-to-close range-based volatility proxies, regarded as more accurate than the close-to-close squared returns: they exclude the noise from the dynamics of the opening jumps and they ensure greater accuracy in volatility forecasting through the range information they provide (see Chou et al. 2010, 2015, Molnár, 2012 and the references therein). Therefore, we incorporate the GK variable in our HEAVY system, in order to improve the model's forecasting performance.

Table 3 presents the five stock indices extracted from the database and provides volatility estimations for each one's squared returns, realized variances, and GK volatilities time series for the respective sample period (see also the DJ series graphs in Appendix B, Figures A.1-A.4). We calculate the standard deviation of the series and the annualized volatility. Annualized volatility is the square rooted mean of 252 times the squared return or the realized variance. The standard deviations are always lower than the annualized volatilities. The realized variances and the GK volatilities have lower annualized volatilities and standard deviations than the squared returns since they ignore the overnight effects and are affected by less noise. The returns represent the close-to-close yield, the realized variance the open-to-close variation, and the GK volatility the open-to-close range-based variation. The annualized volatility of the realized and GK measure is between 10% and 18%, while the squared returns show figures from 14% to 24%.

Table 3. Data Description

	Sample period			r_t^2		RV_t		GK_t	
Index	Start date	End date	Obs.	Avol	sd	Avol	sd	Avol	sd
DJ	03/01/2000	27/09/2019	4950	0.178	0.040	0.165	0.026	0.145	0.022
KOSPI	04/01/2000	30/09/2019	4857	0.235	0.067	0.174	0.022	0.170	0.027
CAC	03/01/2000	30/09/2019	5034	0.222	0.052	0.182	0.022	0.175	0.021
AORD	04/01/2000	30/09/2019	4985	0.143	0.022	0.108	0.008	0.100	0.009
IPC	03/01/2000	30/09/2019	4953	0.202	0.044	0.144	0.018	0.155	0.017

Notes: Avol is the annualized volatility and sd is the standard deviation.

Next, we examine the sample autocorrelations of the power transformed absolute returns $|r_t|^{\delta_r}$, signed square rooted realized variance $|SSR\_RM_t|^{\delta_R}$, and GK volatility $|SSR\_GK_t|^{\delta_g}$, for various values of δ_i. Figures 2, 3, and 4 show the autocorrelograms of the Dow Jones index from lag 1 to 120 for $\delta_r = 1.3, 1.7, 2.0$, $\delta_R = 1.1, 1.5, 2.0$, and $\delta_g = 1.0, 1.5, 2.0$ (similar autocorrelograms for the other four

indices available upon request). The sample autocorrelations for $|r_t|^{1.3}$ are greater than the sample autocorrelations of $|r_t|^{\delta_r}$ for $\delta_r = 1.7, 2.0$ at every lag up to at least 120 lags. In other words, the most interesting finding from the autocorrelogram is that $|r_t|^{\delta_r}$ has the strongest and slowest decaying autocorrelation when $\delta_r = 1.3$. Similarly, for the realized measure and GK volatility, the powers with the strongest autocorrelation function are $\delta_R = 1.1$ and $\delta_g = 1.0$, respectively. Furthermore, Figures 5, 6, and 7 present the sample autocorrelations of $|r_t|^{\delta_r}$, $|SSR\_RM_t|^{\delta_R}$, and $|SSR\_GK_t|^{\delta_g}$ as a function of δ_i for lags $1, 12, 36, 72$ and 96. For example, for lag 12, the highest autocorrelation values of power transformed absolute returns and signed square rooted realized and GK volatility are calculated closer to the power of 1.5 and 1.0, respectively. These figures explain our motivation to extend the benchmark HEAVY through the APARCH framework of Ding et al. (1993) and confirm the power choice of our econometric models, which is $\delta_r = 1.3$ for returns, $\delta_R = 1.1$ for the realized measure, and $\delta_g = 1.0$ for GK volatility (see Section 4).

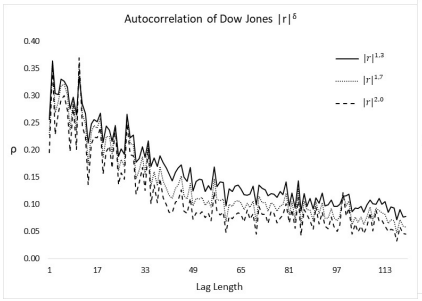

Figure 2. Autocorrelation of Dow Jones $|r_t|^{\delta_r}$ for $\delta_r = 1.3, 1.7, 2.0$

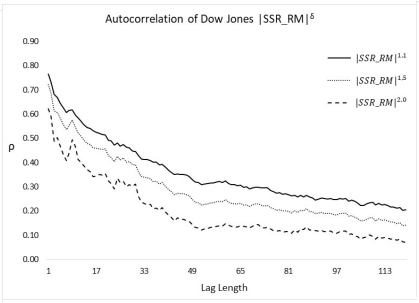

Figure 3. Autocorrelation of Dow Jones $|SSR\_RM_t|^{\delta_R}$ for $\delta_R = 1.1, 1.5, 2.0$

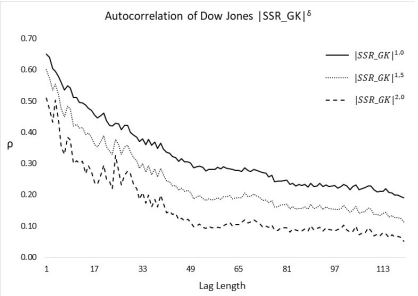

Figure 4. Autocorrelation of Dow Jones $|SSR\_GK_t|^{\delta_g}$ for $\delta_g = 1.0, 1.5, 2.0$

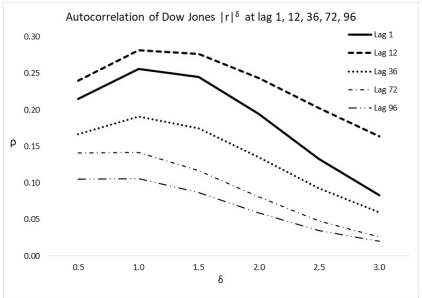

Figure 5. Autocorrelation of Dow Jones $|r_t|^{\delta_r}$ at lags $1, 12, 36, 72, 96$

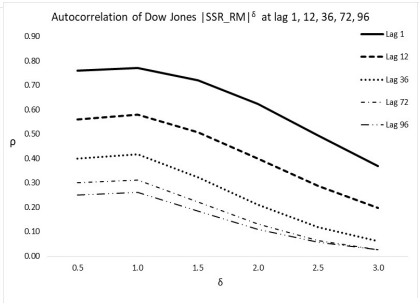

Figure 6. Autocorrelation of Dow Jones $|SSR\_RM_t|^{\delta_R}$ at lags $1, 12, 36, 72, 96$

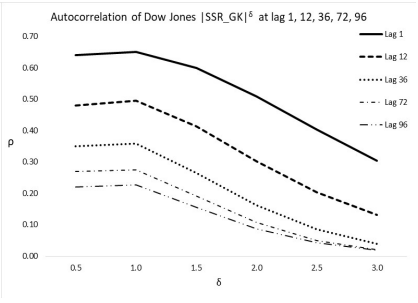

Figure 7. Autocorrelation of Dow Jones $|SSR\_GK_t|^{\delta_g}$ at lags $1, 12, 36, 72, 96$

4.2 Estimated Models

Building upon the introduction of the GARCH-X process by Engle (2002b) to include realized measures as exogenous regressors in the conditional variance equation, Han and Kristensen (2014) and Han (2015) studied the asymptotic properties of this new specification with a fractionally integrated (nonstationary) process included as covariate (see also Francq and Thieu, 2019). Moreover, Nakatani and Teräsvirta (2009) and Pedersen (2017) focused on the multivariate case, the so-called extended constant conditional correlation, which allows for volatility spillovers and they developed inference and testing for the QMLE parameters (see also Ling and McAleer, 2003 for the asymptotic theory of vector ARMA-GARCH processes). For the extended HEAVY models, we employ the existing Gaussian QMLE and multistep-ahead predictors applied in the APARCH framework (see, for example, He and Teräsvirta 1999, Laurent, 2004, Karanasos and Kim, 2006, and the theoretical properties derived in Section 3). Following Pedersen and Rahbek (2019), we first test for arch effects and after rejecting the conditional homoscedasticity hypothesis we apply one-sided significance tests of the covariates added to the estimated GARCH processes.

We first estimate the bivariate benchmark formulation as in Shephard and Sheppard (2010), that is, without asymmetries and power transformations, obtaining very similar results (Table 4). For the benchmark specification, the only unconditional regressor in both equations is the first lag of the RM_t. In other words, the chosen returns equation is a GARCH$(1,0)$-X process leaving out the own Arch effect, α_{rr}, from lagged squared returns since it becomes insignificant when we add the cross effect of the lagged realized measure as regressor, with a Heavy coefficient, α_{rR}, high in value and significance across all indices. The momentum parameter, β_r, is estimated around 0.44 to 0.84. For the SSR realized variance, the best-chosen model is the GARCH$(1,1)$ without the cross effect from lagged squared returns. The Heavy term, α_{RR}, is estimated between 0.25 and 0.47 and the momentum, β_R, is around 0.53 to 0.74. The benchmark system of equations chosen (three alternative GARCH models are tested for each dependent variable with order: $(1,1)$, $(1,0)$-X, and the most general one, that is, $(1,1)$-X) is the same as in Shephard and Sheppard (2010) with similar parameter values and the identical conclusion that the realized measure of variation does all the work of moving around the conditional variances of stock returns and the SSR realized variance. The benchmark's conclusion, as we show in this study, does not hold for the more richly parametrized asymmetric power model. More importantly, according to the SBT statistics, the asymmetric effect is obviously omitted from the benchmark specification with the sign coefficient always significant (p-values lower than 0.02).

Table 4. The Benchmark HEAVY model

	DJ	KOSPI	CAC	AORD	IPC
Panel A: Stock Returns, HEAVY-r					
$(1-\beta_r L)\sigma^2_{rt} = \omega_r + \alpha_{rR} L(RM_t)$					
β_r	0.65 (15.99)***	0.67 (10.58)***	0.44 (7.68)***	0.78 (26.61)***	0.84 (28.45)***
α_{rR}	0.39 (7.62)***	0.62 (5.27)***	0.82 (9.05)***	0.37 (6.88)***	0.25 (5.17)***
Q_{12}	15.43 [0.22]	12.94 [0.37]	12.05 [0.44]	14.40 [0.28]	15.40 [0.21]
SBT	3.07 [0.00]	2.32 [0.02]	2.29 [0.02]	2.60 [0.01]	4.91 [0.00]
lnL	−6336.82	−7599.64	−7762.45	−5728.74	−7582.94
Panel B: Realized Measure, HEAVY-R					
$(1-\beta_R L)\sigma^2_{Rt} = \omega_R + \alpha_{RR} L(RM_t)$					
β_R	0.57 (14.06)***	0.53 (13.11)***	0.57 (17.08)***	0.74 (30.57)***	0.67 (11.56)***
α_{RR}	0.44 (9.26)***	0.47 (10.59)***	0.42 (12.40)***	0.25 (10.45)***	0.33 (5.19)***
Q_{12}	12.52 [0.41]	16.20 [0.18]	9.54 [0.66]	16.77 [0.16]	16.23 [0.17]
SBT	3.68 [0.00]	3.49 [0.00]	2.25 [0.02]	2.47 [0.01]	2.99 [0.00]
lnL	−5930.41	−6140.66	−6819.26	−4362.39	−5823.11

Notes: The numbers in parentheses are t-statistics. ***, **, * denote significance at the 0.01, 0.05, 0.10 level, respectively. Q_{12} is the Box-Pierce Q-statistics on the standardized residuals with 12 lags. SBT denotes the Sign Bias test of Engle and Ng (1993). lnL denotes the log-likelihood value for each specification. The numbers in square brackets are p-values.

Moving to our proposed extension of the benchmark bivariate system, Tables 5A-5C present the estimation results for the chosen three-dimensional asymmetric power specifications (see also the 3D-Benchmark model in Appendix C, Table A.1). Wald and t-tests are used to test the significance of the Heavy, Arch, and Garman parameters, rejecting the null hypothesis at 10% in all cases. We should highlight the fact that since all the parameters take non-negative values, we use one-sided tests (see, for example, Pedersen and Rahbek, 2019).

For all three dependent variables, we statistically prefer the double asymmetric power (DAP) specification since most power transformed conditional variances are significantly affected by own and cross asymmetries. KOSPI's realized measure equation is the only case where we prefer the cross asymmetric

power (CAP) model since own asymmetries are insignificant and therefore excluded. Furthermore, we estimate the power terms separately with a two-stage procedure, as follows: We, first, estimate univariate asymmetric power specifications for the returns, the realized measure, and GK volatility. The Wald tests for the estimated power terms (available upon request) reject the hypothesis of $\delta_i = 2$ in all cases. In the second stage, we use the estimated powers, δ_r, δ_R, and δ_g, from the first step to power transform each series' conditional variance and incorporate them into the trivariate model. The sequential procedure produces the fixed power term values, which are the same for the three specifications (δ_r, δ_R, and δ_g are common for Panels A, B, and C).

For the returns, the estimated power, δ_r, is between 1.30 and 1.60 (see Table 5A). The Heavy asymmetry parameter, γ_{rR}, is significant and around 0.06 (min. value) to 0.13 (max. value). Although α_{rr} is insignificant and excluded in all cases, the own asymmetry parameter is significant with $\gamma_{rr} \in [0.08, 0.11]$. In addition, the cross Garman parameter, α_{rg}, is significant and $0.07 \leq \alpha_{rg} \leq 0.13$ in all cases. In other words, the lagged values of all three powered variables, that is, the negative signed realized measure, the squared negative returns, and the GK volatility, drive the model of the power transformed conditional variance of returns. Moreover, the momentum parameter, β_r, is estimated to be around 0.80 to 0.90. Obviously, all five indices generated very similar DAP specifications.

Table 5A. The 3D-DAP-HEAVY model

	DJ	KOSPI	CAC	AORD	IPC
	Panel A: Stock Returns				
	$(1-\beta_r L)(\sigma_{rt}^2)^{\frac{\delta_r}{2}} = \omega_r + \gamma_{rr} s_{t-1} L(r_t^2)^{\frac{\delta_r}{2}} +$ $\gamma_{rR} s_{t-1} L(RM_t)^{\frac{\delta_R}{2}} + \alpha_{rg} L(GK_t)^{\frac{\delta_g}{2}}$				
β_r	0.81 (45.11)***	0.82 (25.25)***	0.80 (24.33)***	0.87 (55.05)***	0.91 (65.59)***
α_{rg}	0.10 (4.78)***	0.13 (4.66)***	0.12 (3.19)***	0.08 (3.83)***	0.07 (3.99)***
γ_{rr}	0.08 (5.08)***	0.09 (4.84)***	0.10 (6.00)***	0.09 (6.46)***	0.11 (8.39)***
γ_{rR}	0.10 (4.76)***	0.12 (3.48)***	0.13 (4.32)***	0.07 (2.76)***	0.06 (3.90)***
δ_r	1.30	1.50	1.40	1.60	1.60
δ_R	1.10	1.20	1.10	1.30	1.00
δ_g	1.00	1.20	1.10	1.20	1.20
Q_{12}	15.89 [0.20]	11.64 [0.48]	15.12 [0.24]	13.73 [0.19]	8.12 [0.62]
SBT	1.16 [0.24]	0.84 [0.40]	0.31 [0.75]	0.41 [0.68]	0.11 [0.91]
lnL	−5974.12	−6933.25	−7078.02	−5584.51	−6890.68

Notes: See notes in Table 4.

Similarly, for the realized measure the most preferred specification is the DAP one in most cases, as the estimated power is $\delta_R \in [1.00, 1.30]$ (see Table 5B). Both Heavy parameters, α_{RR} and γ_{RR}, are mostly significant: α_{RR} is around 0.05 (min. value) to 0.27 (max. value), while γ_{RR}, is between 0.03 and 0.05. Only for the KOSPI index, the own asymmetries are insignificant and excluded. Moreover, the cross Arch asymmetry parameter is significant with $\gamma_{Rr} \in [0.04, 0.09]$, as well as the cross Garman parameter, α_{Rg}, (with estimated values between 0.05 and 0.12). This means that the power transformed conditional variance of $\widetilde{RM}_t$ is significantly affected by the lagged values of all three powered variables: squared negative returns, realized measure, and GK volatility. Lastly, the momentum parameter, β_R, is estimated to be around 0.62 to 0.81.

Table 5B. The 3D-DAP-HEAVY model

	DJ	KOSPI	CAC	AORD	IPC
	Panel B: Realized Measure				
	$(1-\beta_R L)(\sigma_{Rt}^2)^{\frac{\delta_R}{2}} = \omega_R +$				
	$(\alpha_{RR} + \gamma_{RR} s_{t-1}) L(RM_t)^{\frac{\delta_R}{2}} +$				
	$\gamma_{Rr} s_{t-1} L(r_t^2)^{\frac{\delta_r}{2}} + \alpha_{Rg} L(GK_t)^{\frac{\delta_g}{2}}$				
β_R	0.71 $(41.14)^{***}$	0.62 $(25.07)^{***}$	0.72 $(36.11)^{***}$	0.81 $(47.29)^{***}$	0.73 $(31.23)^{***}$
α_{RR}	0.10 $(5.62)^{***}$	0.27 $(12.04)^{***}$	0.16 $(7.57)^{***}$	0.05 $(3.43)^{***}$	0.19 $(9.48)^{***}$
α_{Rg}	0.12 $(7.94)^{***}$	0.06 $(3.83)^{***}$	0.05 $(4.38)^{***}$	0.08 $(5.96)^{***}$	0.05 $(4.33)^{***}$
γ_{RR}	0.05 $(5.09)^{***}$		0.03 $(3.61)^{***}$	0.04 $(4.60)^{***}$	0.03 $(2.82)^{***}$
γ_{Rr}	0.08 $(8.23)^{***}$	0.04 $(9.44)^{***}$	0.05 $(11.25)^{***}$	0.04 $(6.75)^{***}$	0.09 $(5.74)^{***}$
δ_R	1.10	1.20	1.10	1.30	1.00
δ_r	1.30	1.50	1.40	1.60	1.60
δ_g	1.00	1.20	1.10	1.20	1.20
Q_{12}	15.18 [0.23]	14.40 [0.28]	15.16 [0.23]	13.72 [0.19]	13.68 [0.20]
SBT	0.64 [0.52]	0.71 [0.48]	0.74 [0.46]	1.01 [0.31]	1.12 [0.26]
lnL	−5264.81	−5346.23	−5865.78	−4151.74	−5230.93

Notes: See notes in Table 4.

Finally, regarding the GK volatility the DAP specification is again the chosen one (see Table 5C). In particular, the own power term is $1.00 \leq \delta_g \leq 1.20$ in all cases. In addition, the Heavy (α_{gR}), the own asymmetry, γ_{gg}, and the Arch asymmetry, γ_{gr}, parameters are significant in all cases. In other words, the first lags of all three powered variables (realized measure, negative signed GK volatility, and squared negative returns) drive the model of the power transformed conditional variance of $\widetilde{GK}_t$.

Table 5C. The 3D-DAP-HEAVY model

	DJ	KOSPI	CAC	AORD	IPC
	Panel C: GK volatility				
	$(1-\beta_g L)(\sigma_{gt}^2)^{\frac{\delta_g}{2}} = \omega_g + \gamma_{gg} L(GK_t)^{\frac{\delta_g}{2}} +$ $\alpha_{gR} s_{t-1} L(RM_t)^{\frac{\delta_R}{2}} + \gamma_{gr} s_{t-1} L(r_t^2)^{\frac{\delta_r}{2}}$				
β_g	0.76 (35.34)***	0.65 (18.49)***	0.75 (28.51)***	0.82 (44.50)***	0.84 (42.41)***
α_{gR}	0.11 (8.07)***	0.26 (9.18)***	0.16 (7.44)***	0.09 (7.93)***	0.09 (5.57)***
γ_{gg}	0.07 (7.87)***	0.02 (1.77)*	0.05 (5.82)***	0.03 (3.52)***	0.03 (3.11)***
γ_{gr}	0.05 (6.62)***	0.05 (7.85)***	0.04 (8.33)***	0.04 (6.83)***	0.05 (8.66)***
δ_g	1.00	1.20	1.10	1.20	1.20
δ_r	1.30	1.50	1.40	1.60	1.60
δ_R	1.10	1.20	1.10	1.30	1.00
Q_{12}	13.70 [0.32]	14.98 [0.24]	15.04 [0.24]	13.75 [0.30]	13.72 [0.31]
SBT	0.78 [0.44]	0.91 [0.36]	1.16 [0.25]	0.90 [0.37]	1.08 [0.28]
lnL	−4990.36	−5213.30	−5677.71	−3421.67	−5838.98

Notes: See notes in Table 4.

Overall, our results show strong Heavy effects (captured by the γ_{rR}, α_{RR}, γ_{RR} and α_{gR} parameters), asymmetric Arch influences (as the estimated γ_{rr}, γ_{Rr} and γ_{gr} are significant), as well as Garman impacts (captured by the α_{rg}, α_{Rg} and γ_{gg} parameters). According to the log-likelihood (lnL) values reported, the log-likelihood is always higher for the DAP specifications compared to the benchmark ones, that is without asymmetries and powers, proving the superiority of our model's in-sample estimation. The SBT statistics further show that the asymmetric effect is not omitted any more since the sign coefficients are insignificant, with p-values consistently higher than 0.24 (see also the Supplementary Appendix on the empirical application of the trivariate AP specification with long memory [Section A] and structural breaks [Section B]).

Lastly, we estimated the trivariate system of the extended HEAVY models with four alternative correlation models:the CCC-Constant Conditional Correlations (Bollerslev, 1990), the DCC-Dynamic Conditional Correlations (Engle, 2002a), the ADCC-Asymmetric Dynamic Conditional Correlations (Cappiello et al., 2006) and the DECO-Dynamic Equicorrelations (Engle and Kelly, 2012). For simplicity, hereafter, we will assume that $\delta_i = 2$ for all $i = 1, \ldots, N$. The conditional covariance matrix for the N-dimensional vector $\mathbf{r}_t$, $\mathbf{H}_t$ (see Section 3.2, as well), when the conditional correlation matrix is time-varying and is

denoted by $\mathbf{R}_t$, can be written as:

$$\mathbf{H}_t = \mathbf{\Sigma}_t \mathbf{R}_t \mathbf{\Sigma}_t,$$

where the elements occupying the off-diagonal entries of $\mathbf{R}_t$ are given by $\rho_{ij,t} = \sigma_{ij,t}/\sigma_{it}\sigma_{jt}$ for $i \neq j$. In our HEAVY model, we initially assumed that the conditional covariances and dynamic correlations are zero: $\rho_{ij,t} = \sigma_{ij,t} = 0$ for all t and $i \neq j$. This implies that $\mathbf{R}_t = \mathbf{I}$ and $\mathbf{H}_t$ is a diagonal matrix ($\mathbf{H}_t = \mathbf{\Sigma}_t^2$). Allowing for non-zero conditional correlations does not alter our estimation results because the estimation of various non-zero correlation models-the four alternative specifications, namely the CCC, DCC, ADCC, and DECO-is a two-step procedure, where in the first step the parameters in the $\mathbf{\Sigma}_t$ matrix are estimated using the conditional variance equations, while the second step consists of estimating the (off-diagonal) parameters in $\mathbf{R}_t$ (or $\mathbf{R}$ for the CCC case). To see this more explicitly, we present the quasi-likelihood (QL) function. But first, note that $\mathbf{r}_t$ can be written as (see eq. 4):

$$\mathbf{r}_t = \mathbf{Z}_t \boldsymbol{\sigma}_t = \mathbf{\Sigma}_t \mathbf{e}_t, \text{ or equivalently } \mathbf{e}_t = \mathbf{\Sigma}_t^{-1} \mathbf{r}_t.$$

Then QL is given by

$$\begin{aligned} QL &= QL_1 + QL_2 \\ &= \underbrace{-\sum_{t=1}^{T} (n \log(2\pi) + 2 \log |\mathbf{\Sigma}_t| + \mathbf{r}_t' \mathbf{\Sigma}_t^{-2} \mathbf{r}_t)}_{QL_1} \underbrace{- \sum_{t=1}^{T} (\log |\mathbf{\Sigma}_t| + \mathbf{e}_t' \mathbf{R}_t^{-1} \mathbf{e}_t + \mathbf{e}_t' \mathbf{e}_t)}_{QL_2}. \end{aligned}$$

Thus in the first step the parameters of the various extensions of the multivariate HEAVY process are estimated using QL_1, and in the second step we estimate the off-diagonal element in $\mathbf{R}_t$ using the standardized residuals: $\widehat{\mathbf{e}}_t = \widehat{\mathbf{\Sigma}}_t^{-1} \mathbf{r}_t$ in QL_2. In all cases, the three alternative dynamic models (DCC, ADCC and DECO) estimate the average conditional correlations for the three volatility measures around 0.75 to 0.95 similar to the CCC constant correlation values.

All in all, the conditional correlations extension does not improve further the 3D-DAP-HEAVY formulation since it provides identical results for the conditional variance equations and estimates similar correlation levels for all indices' formulations (results not reported but available upon request).

5 Forecast Evaluation

Following the in-sample estimation of the proposed extensions to the HEAVY system of equations, we perform multistep-ahead out-of-sample forecasting in order to compare the forecasting accuracy of the enriched specifications proposed in this study with the benchmark model introduced by Shephard and Sheppard (2010). We compute 1-, 5-, 10-, and 22-step-ahead forecasts of the (power transformed) conditional variances for the benchmark and the 3D-DAP models. We apply a rolling window in-sample

estimation using 2500 observations (the initial in-sample estimation period for DJ spans from 3/1/2000 until 24/12/2009). Each model is re-estimated daily based on the 2500-day rolling sample. The resulted out-of-sample forecasts of each specification calculated for DJ are as follows: 2450 one-step-ahead, 2446 five-step-ahead, 2441 ten-step-ahead, and 2439 twenty-two-step-ahead forecasted variances.

We then use the time series of the forecasted values to compute the Mean Square Error (MSE) and the QLIKE Loss Function (Patton, 2011) of each point forecast compared to the respective actual value. For each formulation and each forecast horizon, we calculate the average MSE and QLIKE to build the ratio of the forecast losses for each extended HEAVY specification to the loss of the benchmark one. A ratio lower than the unity indicates the forecasting superiority of the proposed models relative to the benchmark one. The lowest ratio means lowest forecast losses, that is the model with the best forecasting performance. Based on the MSE calculations, we further apply the test for the pairwise comparison of nested models (here the benchmark specification vs the AP extensions) suggested by Harvey, Leybourne, and Newbold (1998), HLN thereafter. The HLN forecast encompassing test was introduced as a modification to the Diebold-Mariano test (Diebold and Mariano, 1995) to account for the fact that models are nested (here the 3D-DAP nests the benchmark specification). HLN test whether the differences between the two competing formulations' forecasts are statistically significant and the larger model's forecast losses are lower than the nested model's ones (see also Clark and McCracken, 2001).

We apply the optimal predictor $|\mathbf{r}_t|^{\wedge\boldsymbol{\delta}}$ (under Proposition 3 in Section 3.2.3) and calculate the out-of-sample forecasts. The results, presented in Tables 6 and 7 for the DJ index (similar forecasting results for the other four indices available upon request), clearly show the preference for our extensions over the benchmark models across all time horizons. The 3D-DAP specification dominates the benchmark model with the lowest MSE and QLIKE (Table 6). Given the HLN test, the Asymmetric Power formulation performs significantly better than the benchmark HEAVY model in the short- and long-term horizons, with the computed forecasts significantly closer to the actual values for the enriched HEAVY formulations. HLN test results reject the null hypothesis of equal forecasts in favor of the 3D-DAP model's lower forecast losses at 5% significance level (Table 7). Investors, traders and risk managers can benefit from the superior short-term forecasts for one up to ten days, while policymakers should focus on the longer-term forecasting performance to predict 'safely' the one-month-forward financial volatility given the significant range-based effects.

Table 6. Mean Square Error (MSE) and QLIKE of m-step-ahead out-of-sample forecasts for DJ as a Ratio of the benchmark model and HLN test.

	MSE				QLIKE			
Specifications↓ m-steps →	1	5	10	22	1	5	10	22
Panel A: Stock Returns (HEAVY-r)								
Benchmark (bivariate)	1.000	1.000	1.000	1.000	1.000	1.000	1.000	1.000
3D-DAP	**0.769**	**0.791**	**0.824**	**0.872**	**0.711**	**0.747**	**0.761**	**0.833**
Panel B: Realized Measure (HEAVY-R)								
Benchmark (bivariate)	1.000	1.000	1.000	1.000	1.000	1.000	1.000	1.000
3D-DAP	**0.784**	**0.836**	**0.845**	**0.946**	**0.721**	**0.744**	**0.780**	**0.865**
Panel C: GK volatility (HEAVY-g)								
Benchmark$^{\oplus}$	1.000	1.000	1.000	1.000	1.000	1.000	1.000	1.000
3D-DAP	**0.804**	**0.773**	**0.850**	**0.912**	**0.832**	**0.741**	**0.841**	**0.897**

Notes: Bold numbers indicate minimum values across the different specifications.

$^{\oplus}$The Benchmark Heavy-g specification is defined in Table A.1, Panel C (Trivariate Benchmark)

Table 7. HLN Forecast encompassing test results for DJ (p-values).

Specifications↓ m-steps →	1	5	10	22
Panel A: Stock Returns (HEAVY-r)				
Benchmark vs 3D-DAP	0.011	0.019	0.033	0.041
Panel B: Realized Measure (HEAVY-R)				
Benchmark vs 3D-DAP	0.017	0.022	0.036	0.053
Panel C: GK volatility (HEAVY-g)				
Benchmark vs 3D-DAP	0.020	0.015	0.038	0.046

Notes: The numbers reported are p-values of the HLN (1998) test of the null hypothesis for equal forecasting performance against the one-sided alternative that the 3D-DAP outperforms the nested benchmark specification.

The forecasting performance of the proposed models can be further examined in a real-world risk management empirical example. Value-at-Risk (VaR) is a daily metric for market risk measurement, defined as the potential loss in the value of a portfolio, over a pre-defined holding period, for a given confidence level. The most important input in the VaR calculation is the one-day volatility forecast of the risk factor relevant to the trading portfolio under scope. We directly apply our conditional variance

forecasts in a long portfolio position to one Dow Jones Industrial Average index contract starting from 7/5/2019. We calculate 100 daily VaR values from 8/5/2019 to 27/9/2019 using the one-day conditional variance forecasts of each model for returns and realized measure (4 models in total). Given that the conditional mean return is zero and the returns follow the normal distribution, we, first, calculate the one-day VaR with 99% and 95% confidence level. According to the parametric approach to VaR calculation, we multiply the daily portfolio value with the one-day-ahead conditional volatility forecast (equal to the square root of the conditional variance forecast) and the left quantile at the respective confidence level of the normal distribution (the z-scores for 99% and 95% confidence level are 2.326 and 1.645, respectively). Secondly, we calculate the daily realized return of the portfolio (gains and losses) and, thirdly, we perform the backtesting exercise, comparing the realized returns with the respective one-day VaR for the 99% and 95% confidence levels. In the cases where the realized loss exceeds the respective day's VaR value, we record it as an exception in the backtesting procedure, meaning that the VaR metric fails to cover the loss of the specific day's portfolio value.

According to the backtesting results (see Table 8: Backtesting results, No. of Exceptions), the number of exceptions across all models is in line with the selected confidence level (the 99% and 95% confidence levels allow for 1 and 5 exceptions, respectively, every 100 days) and low enough to prevent supervisors from increasing the capital charges (in which case we refer to a bank's trading portfolio). The higher number of exceptions means higher market risk capital requirements for financial institutions since regulators heavily penalize banks' internal models that fail to cover trading losses through the VaR estimates. Following the Basel traffic light approach, the market risk capital charge increases when the backtesting exceptions are more than 4 in a sample of 250 daily observations and 99% confidence level. Since all models provide adequate coverage of the realized losses, we should further compare the average and minimum VaR estimates calculated based on the forecasts of each specification (Table 8: Descriptive statistics). The VaR estimate that provides the higher loss coverage with the lower capital charges is the one with the lower minimum and higher mean values. This is achieved by the realized measure specifications, where we prefer the asymmetric power model, augmented with the range-based volatility impact. Given that the market risk capital requirement is calculated on the trading portfolio total 99% VaR (absolute value, 60-day average) adjusted by the penalty of the backtesting exceptions (higher than 4 in the 250-day sample), the bank needs the smallest possible VaR average with the larger minimum estimate in absolute terms. Thereupon, our proposed models clearly satisfy both criteria, contributing to the risk manager's VaR calculation of the volatility forecasts that better capture the loss distribution (higher extreme loss coverage with higher absolute minimum value) without inflating the capital charges (lower absolute mean).

Table 8. VaR Backtesting results and Descriptive statistics for the DJ portfolio.

	Backtesting results		Descriptive statistics			
	No. of Exceptions		99% VaR		95% VaR	
Specifications	99% VaR	95% VaR	Mean	Min.	Mean	Min.
Panel A: Stock Returns (HEAVY-r)						
Benchmark (bivariate)	1	3	-700.04	$-1,418.87$	-494.97	$-1,003.22$
3D-DAP	1	3	-656.75	$-1,346.29$	-468.80	-951.90
Panel B: Realized Measure (HEAVY-R)						
Benchmark (bivariate)	1	3	-632.24	-934.48	-447.03	-660.72
3D-DAP	1	3	$\mathbf{-641.20}$	$\mathbf{-1,241.32}$	-456.90	-877.68

Notes: Mean and Min. denote the average and minimum VaR estimate, respectively. Bold numbers indicate the preferred specifications for the lower market risk capital charge with the higher loss coverage.

Furthermore, the volatility forecasts produced by the 3D-DAP-HEAVY model are directly applicable to a wide range of business finance operations, alongside the well-established risk management practice outlined in the VaR empirical exercise. Portfolio managers should rely on the proposed framework to predict future volatility in asset allocation and minimum-variance portfolio selection complying with their clients' risk appetite. Risk-averse investors' mandates specify low volatility boundaries on their portfolio positions, while risk lovers allow for higher volatilities on the risk-return trade-off of their investments. Accurate volatility predictions can also be used in a forward-looking performance evaluation context, through the risk-adjusted metrics, i.e. the Sharpe or the Treynor risk-adjusted return ratios. Traders and risk managers focus on the volatility trajectory in derivatives pricing, volatility targeting strategies, and several other trading decisions. Trading and hedging in financial markets depend on risk factors whose predicted volatilities are the main input of any pricing function applied. Moreover, financial chiefs consider volatility forecasts when they decide on investment projects or funding choices (bond and equity valuation defining the cost of capital) given that expected future cash-flow variation is a critical factor in business analytics.

Finally, policymakers and authorities supervising and regulating the financial system should take into account reliable volatility forecasts in designing macro- and micro-prudential policy responses. The risk management of the financial system is structured as follows: i) identification of risk sources (both endogenous - financial market volatility - and exogenous - the macroeconomy), ii) assessment of the nature of risk factors, iii) risk measurement (micro-prudential metrics at the financial institution level and macro-prudential metrics at the system and markets level), and iv) risk mitigation with proactive regulation and crisis preparedness plans and strategies. Therefore, regulators should employ the range-

informed financial volatility forecasts of the 3D-DAP-HEAVY model across the whole risk management process and the financial stability oversight tools, such as the early warning systems, the macro stress-tests on financial institutions and the bank capital and risk frameworks. For example, the macro stress-test scenario inputs, which include, among others, stock market volatility predictions for the financial institutions' trading books, should consider range-informed volatility estimates. Furthermore, complying with the capital and risk frameworks set by supervisors (Basel committee and central banks), financial institutions measure their trading portfolio's market risk (beyond the credit risk of their loan portfolio) with the daily Value-at-Risk (VaR) metric. Given that reliable volatility forecasts, provided by our superior modeling framework, improve the VaR estimates considerably, supervisors should encourage banks to improve their market risk internal models with more accurate range-informed volatility forecasts based on both low- and high-frequency data.

6 Conclusions

Our study has extended the bivariate HEAVY system to the three-dimensional DAP specification. Our major contribution to volatility modeling research within this HEAVY framework is twofold: We, firstly, augment the benchmark model with a third variable, that is the range-based volatility, in order to achieve greater accuracy in volatility forecasting. Secondly, we enrich the trivariate formulation by taking into consideration leverage and power characteristics. Thirdly, we derive the theoretical time series properties (optimal predictors and second moment structure) of the multivariate asymmetric power system and assess its finite-sample performance through a simulation study. Our empirical results favor the most general asymmetric power specification, where the lags of all three powered variables - squared negative returns, GK volatility, and realized variance - move the dynamics of each power transformed conditional variance. The asymmetric response to negative and positive shocks and its power transformations ensure the superiority of our contribution, which can be implemented on the areas of asset allocation and portfolio selection, as well as on several risk management practices. Further, we provide evidence on the forecasting superiority of our extensions over the benchmark HEAVY model through the rolling window out-of-sample forecasting across multiple short- and long-term horizons.

Our empirical findings on the nexus between low-frequency daily squared returns, range-based volatility, and high-frequency intra-daily realized measures, provide a volatility forecasting framework with important implications for policymakers and market practitioners, from investors, risk and portfolio managers up to financial chiefs, leaving ample room for future research on further model extensions. Thereupon, policymakers and market players should use our HEAVY framework to closely watch and forecast financial volatility patterns in the process of devising drastic policies, enforcing the financial

system's regulations to preserve financial stability, deciding on asset allocation, hedging strategies, and investment projects. As part of future research, it would be interesting to extend the theoretical framework of the asymmetric power system with long memory features and structural breaks (supporting our empirical illustrations in the Supplementary Appendix). A further interesting line of future research could be the enrichment of the multivariate HEAVY formulation of Noureldin et al. (2012) with leverage, power transformations, and long memory, extending the recent study of Dark (2018), who has applied a long memory multivariate GARCH model to the multivariate HEAVY, or Opschoor et al. (2018) within the Generalized Autoregressive Score (GAS) process of Creal et al. (2013).

Data Availability Statement

The data that support the findings of this study are publicly available in the Oxford-Man Institute Realized Library at https://realized.oxford-man.ox.ac.uk/data/download.

References

[1] Andersen, T.G., Bollerslev, T., 1998. Answering the skeptics: Yes, standard volatility models do provide accurate forecasts. International Economic Review 39, 885-905.

[2] Andersen, T.G., Bollerslev, T., Diebold, F.X., Labys, P., 2001. The distribution of exchange rate volatility. Journal of the American Statistical Association 96, 42-55.

[3] Barndorff-Nielsen, O.E., Hansen, P.R., Lunde, A., Shephard, N., 2008. Designing realized kernels to measure the ex-post variation of equity prices in the presence of noise. Econometrica 76, 1481-1536.

[4] Barndorff-Nielsen, O.E., Hansen, P.R., Lunde, A., Shephard, N., 2009. Realized kernels in practice: Trades and quotes. Econometrics Journal 12, C1-C32.

[5] Barndorff-Nielsen, O.E., Shephard, N., 2002. Econometric analysis of realized volatility and its use in estimating stochastic volatility models. Journal of the Royal Statistical Society, Series B 64, 253-280.

[6] Bollerslev, T., 1986. Generalized autoregressive conditional heteroskedasticity. Journal of Econometrics 31, 307-327.

[7] Bollerslev, T., 1990. Modelling the coherence in short-run nominal exchange rates: A multivariate generalized ARCH model. Review of Economics and Statistics 72, 498-505.

[8] Borovkova, S., Mahakena, D., 2015. News, volatility and jumps: The case of natural gas futures. Quantitative Finance 15, 1217-1242.

[9] Brooks, R.D., Faff, R.W., McKenzie, M.D., Mitchell, H., 2000. A multi-country study of power ARCH models and national stock market returns. Journal of International Money and Finance 19, 377-397.

[10] Cappiello, L., Engle, R.F., Sheppard, K., 2006. Asymmetric dynamics in the correlations of global equity and bond returns. Journal of Financial Econometrics 4, 537-572.

[11] Chen, Z., Daigler, R., Parhizgari, A., 2006. Persistence of volatility in future markets. Journal of Futures Markets 26, 571-594.

[12] Chou, R.Y., Chou, H., and Liu, N., 2010. Range volatility models and their applications in finance. In Lee, C.-F., and Lee, J.: Handbook of quantitative finance and risk management, 1273-1282. New York, NY: Springer.

[13] Chou, R.Y., Chou, H., and Liu, N., 2015. Range volatility: A review of models and empirical studies. In Lee, C.-F., and Lee, J.: Handbook of financial econometrics and statistics, 2029-2050. New York, NY: Springer.

[14] Clark, T.E., McCracken, M.W., 2001. Tests for equal forecast accuracy and encompassing for nested models. Journal of Econometrics 105, 85-110.

[15] Conrad, C., Karanasos, M., 2010. Negative volatility spillovers in the unrestricted ECCC-GARCH model. Econometric Theory 26, 838-862.

[16] Corsi, F., Mittnik, S., Pigorsch, C., Pigorsch, U., 2008. The volatility of realized volatility. Econometric Reviews 27, 46-78.

[17] Creal, D.D., Koopman, S.J., Lucas, A., 2013. Generalized autoregressive score models with applications. Journal of Applied Econometrics 28, 777-795.

[18] Dark, J.G., 2018. Multivariate models with long memory dependence in conditional correlation and volatility. Journal of Empirical Finance 48, 162-180.

[19] Diebold, F.X., Mariano, R.S., 1995. Comparing predictive accuracy. Journal of Business and Economic Statistics 13, 253-263.

[20] Ding, Z., Granger, C.W.J., Engle, R.F., 1993. A long memory property of stock market returns and a new model. Journal of Empirical Finance 1, 83-106.

[21] Engle, R.F., 2002a. Dynamic conditional correlation: A simple class of multivariate generalized autoregressive conditional heteroskedasticity models. Journal of Business and Economic Statistics 20, 339-350.

[22] Engle, R.F., 2002b. New frontiers for ARCH models. Journal of Applied Econometrics 17, 425-446.

[23] Engle, R.F., Kelly, B.T., 2012. Dynamic equicorrelation. Journal of Business and Economic Statistics 30, 212-228.

[24] Engle, R.F., Ng, V.K., 1993. Measuring and testing the impact of news on volatility. The Journal of Finance 48, 1749-1778.

[25] Garman, M., Klass, M., 1980. On the estimation of security price volatilities from historical data. Journal of Business 53, 67-78.

[26] Francq, C., Thieu, L.Q., 2019. QML inference for volatility models with covariates. Econometric Theory 35, 37-72.

[27] Glosten, L.R., Jagannathan R., Runkle, D.E., 1993. On the relation between the expected value and the volatility of the nominal excess return on stocks. The Journal of Finance 48, 1779-1801.

[28] Halunga, A.G., Orme, C.D., 2009. First-order asymptotic theory for parametric misspecification tests of GARCH models. Econometric Theory 25, 364-410.

[29] Han, H., 2015. Asymptotic properties of GARCH-X processes. Journal of Financial Econometrics 13, 188-221.

[30] Han, H., Kristensen, D., 2014. Asymptotic theory for the QMLE in GARCH-X models with stationary and nonstationary covariates. Journal of Business & Economic Statistics 32, 416-429.

[31] Hansen, P.R., Huang, Z., Shek, H., 2012. Realized GARCH: A joint model for returns and realized measures of volatility. Journal of Applied Econometrics 27, 877-906.

[32] Harvey, D.I., Leybourne, S.J., Newbold, P., 1998. Tests for forecast encompassing. Journal of Business and Economic Statistics 16, 254-259.

[33] He, C., Teräsvirta, T., 1999. Statistical properties of the asymmetric power ARCH model. In: Engle, R.F., White, H. (Eds.), Cointegration, Causality, and Forecasting. Festschrift in Honour of Clive W.J. Granger. Oxford University Press, Oxford, 462-474.

[34] Heber, G., Lunde, A., Shephard, N., Sheppard, K., 2009. Oxford-Man Institute's (OMI's) realized library, Version 0.2. Oxford-Man Institute: University of Oxford.

[35] Huang, Z., Liu, H., Wang, T., 2016. Modeling long memory volatility using realized measures of volatility: A realized HAR GARCH model. Economic Modelling 52, 812-821.

[36] Karanasos, M., Kim, J., 2006. A re-examination of the asymmetric power ARCH model. Journal of Empirical Finance 13, 113-128.

[37] Laurent, S., 2004. Analytical derivates of the APARCH model. Computational Economics 24, 51-57.

[38] Li, Y.N., Zhang, Y., Zhang, C., 2019. Statistical inference for measurement equation selection in the log-RealGARCH model. Econometric Theory 35, 943-977.

[39] Ling, S., McAleer, M., 2003. Asymptotic theory for a vector ARMA-GARCH model. Econometric Theory 19, 280-310.

[40] Lundbergh, S., Teräsvirta, T., 2002. Evaluating GARCH models. Journal of Econometrics 110, 417-435.

[41] Lütkepohl, H., 1996. Handbook of Matrices (Vol. 1). Chichester: Wiley.

[42] Molnár, P., 2012. Properties of range-based volatility estimators. International Review of Financial Analysis 23, 20-29.

[43] Molnár, P., 2016. High-low range in GARCH models of stock return volatility. Applied Economics, 48, 4977-4991.

[44] Nakatani, T., Teräsvirta, T., 2009. Testing for volatility interactions in the constant conditional correlation GARCH model. Econometrics Journal 12, 147-163.

[45] Noureldin, D., Shephard, N., Sheppard, K., 2012. Multivariate high-frequency-based volatility (HEAVY) models. Journal of Applied Econometrics 27, 907-933.

[46] Opschoor, A., Janus, P., Lucas, A., Van Dijk, D., 2018. New HEAVY models for fat-tailed realized covariances and returns. Journal of Business and Economic Statistics 36, 643-657.

[47] Patton, A.J., 2011. Volatility forecast comparison using imperfect volatility proxies. Journal of Econometrics 160, 246-256.

[48] Pedersen, R.S., 2017. Inference and testing on the boundary in extended constant conditional correlation GARCH models. Journal of Econometrics 196, 23-36.

[49] Pedersen, R.S., Rahbek, A., 2019. Testing GARCH-X type models. Econometric Theory 35, 1012-1047.

[50] Shephard, N., Sheppard, K., 2010. Realising the future: forecasting with high-frequency-based volatility (HEAVY) models. Journal of Applied Econometrics 25, 197-231.

A APPENDIX: *S*econd Moments (Proofs)

In this Section we will derive the proofs of Theorems 2 and 3. But first we present the following lemma that we will use in the proofs below.

Lemma 1 *The* $vec\left[\mathbb{E}\left(\mathbf{A}_{t-1}\mathbf{v}_{t-1}\mathbf{v}_{t-1}'\mathbf{A}_{t-1}'\right)\right]$ *is given by*

$$vec\left[\mathbb{E}\left(\mathbf{A}_{t-1}\mathbf{v}_{t-1}\mathbf{v}_{t-1}'\mathbf{A}_{t-1}'\right)\right] \quad = \quad \overline{\mathbf{A}}^{\otimes 2}\widetilde{\mathbf{Z}}\left[\boldsymbol{\gamma}(0)+\boldsymbol{\sigma}^{\otimes 2}\right]. \tag{A.1}$$

Proof. Using the definition of $\mathbf{v}_{t-1}$ in Definition 1(ii) and interchanging the vec and expectation operators, the left hand side of eq. (A.1) takes the form:

$$\mathbb{E}\left\{vec\left[\mathbf{A}_{t-1}\left(|\mathbf{Z}_t|^{\wedge\boldsymbol{\delta}}-\mathbf{Z}\right)\boldsymbol{\sigma}_t^{\wedge\boldsymbol{\delta}}(\boldsymbol{\sigma}_t^{\wedge\boldsymbol{\delta}})'\left(|\mathbf{Z}_t|^{\wedge\boldsymbol{\delta}}-\mathbf{Z}\right)'\mathbf{A}_{t-1}'\right]\right\}.$$

Using the rules of the vec operator (see, for example, Lütkepohl, 1996, Section 7.2) and, under Condition 2, applying the expectation operator, in view of eq. (13) the above expression yields

$$vec\left[\mathbb{E}\left(\mathbf{A}_{t-1}\mathbf{v}_{t-1}\mathbf{v}_{t-1}'\mathbf{A}_{t-1}'\right)\right] \quad = \quad \mathbb{E}\left(\mathbf{A}_{t-1}^{\otimes 2}\right)\mathbb{E}\left(|\mathbf{Z}_t|^{\wedge\boldsymbol{\delta}}-\mathbf{Z}\right)^{\otimes 2}(\boldsymbol{\gamma}(0)+\boldsymbol{\sigma}^{\otimes 2}). \tag{A.2}$$

Since $\mathbb{E}\left(\mathbf{A}_t^{\otimes 2}\right)=\overline{\mathbf{A}}^{\otimes 2}$ and in view of Notation 8, it follows that the right hand-side of eq. (A.2) equals the right hand-side of eq. (A.1) as required. ■

Proof. (**of Theorem 2**) Rewrite the weak VARMA representation, eq. (6), as

$$\boldsymbol{\sigma}_t^{\wedge\boldsymbol{\delta}}=\boldsymbol{\omega}+\mathbf{C}_{t-1}\boldsymbol{\sigma}_{t-1}^{\wedge\boldsymbol{\delta}}+\mathbf{A}_{t-1}\mathbf{v}_{t-1}.$$

Using $\boldsymbol{\omega}=(\mathbf{I}-\mathbf{C})\boldsymbol{\sigma}$ (see eq. (11)) the above equation can be expressed in terms of deviations from the mean:

$$\boldsymbol{\sigma}_t^{\wedge\boldsymbol{\delta}}-\boldsymbol{\sigma}=(\mathbf{C_{t-1}}-\mathbf{C})\boldsymbol{\sigma}+\mathbf{C}_{t-1}(\boldsymbol{\sigma}_{t-1}^{\wedge\boldsymbol{\delta}}-\boldsymbol{\sigma})+\mathbf{A}_{t-1}\mathbf{v}_{t-1}. \tag{A.3}$$

Taking the transpose on both sides of eq. (A.3) yields

$$(\boldsymbol{\sigma}_t^{\wedge\boldsymbol{\delta}}-\boldsymbol{\sigma})'=\boldsymbol{\sigma}'(\mathbf{C_{t-1}}-\mathbf{C})'+(\boldsymbol{\sigma}_{t-1}^{\wedge\boldsymbol{\delta}}-\boldsymbol{\sigma})'\mathbf{C}_{t-1}'+\mathbf{v}_{t-1}'\mathbf{A}_{t-1}'. \tag{A.4}$$

Right-multiplying eq. (A.3) by eq. (A.4) and, under Condition 2, taking expectations on both sides, yields (in view of eq. (13) and ignoring zero terms):

$$\boldsymbol{\Gamma}(0)=\mathbb{E}\left[\mathbf{C}_{t-1}(\boldsymbol{\sigma}_{t-1}^{\wedge\boldsymbol{\delta}}-\boldsymbol{\sigma})(\boldsymbol{\sigma}_{t-1}^{\wedge\boldsymbol{\delta}}-\boldsymbol{\sigma})'\mathbf{C}_{t-1}'\right]+\mathbb{E}\left(\mathbf{A}_{t-1}\mathbf{v}_{t-1}\mathbf{v}_{t-1}'\mathbf{A}_{t-1}'\right). \tag{A.5}$$

Applying the vec operator to both sides of eq. (A.5) yields

$$\boldsymbol{\gamma}(0)=\mathbb{E}\left(\mathbf{C}_t^{\otimes 2}\right)\boldsymbol{\gamma}(0)+vec\left[\mathbb{E}\left(\mathbf{A}_{t-1}\mathbf{v}_{t-1}\mathbf{v}_{t-1}'\mathbf{A}_{t-1}'\right)\right].$$

In view of Lemma 1 and the fact that $\mathbb{E}\left(\mathbf{C}_t^{\otimes 2}\right) = \mathbf{C}^{\otimes 2}$, we have

$$\boldsymbol{\gamma}(0) = \mathbf{C}^{\otimes 2}\boldsymbol{\gamma}(0) + \overline{\mathbf{A}}^{\otimes 2}\widetilde{\mathbf{Z}}\left[\boldsymbol{\gamma}(0) + \boldsymbol{\sigma}^{\otimes 2}\right].$$

Solving the above equation for $\boldsymbol{\gamma}(0)$ gives

$$\boldsymbol{\gamma}(0) = \left(\mathbf{I}_{N^2} - \widetilde{\mathbf{C}}\right)^{-1}\overline{\mathbf{A}}^{\otimes 2}\widetilde{\mathbf{Z}}\boldsymbol{\sigma}^{\otimes 2}$$

($\widetilde{\mathbf{C}}$ is given in eq. (15)), which completes the proof of eq. (16).

Next, rewrite the general solution in eq. (8) as

$$(\boldsymbol{\sigma}_t^{\wedge\boldsymbol{\delta}})' = \sum_{r=1}^{\ell}(\boldsymbol{\omega}' + \mathbf{v}_{t-r}'\mathbf{A}_{t-r}')\mathbf{D}_{t,r-1}' + (\boldsymbol{\sigma}_{\mathbf{t}-\ell}^{\wedge\boldsymbol{\delta}})'\mathbf{D}_{t,\ell}'.$$

Left-multiplying the above equation by $\boldsymbol{\sigma}_{t-\ell}^{\wedge\boldsymbol{\delta}}$, taking expectations on both sides under Condition 2, and using $\mathbb{E}(\mathbf{D}_{t,\ell}) = \mathbf{C}^{\ell}$, see the text next to eq. (9), yields (in view of eq. (13) and ignoring zero terms):

$$\boldsymbol{\Sigma}(\ell) = \boldsymbol{\sigma}\boldsymbol{\omega}'[(\mathbf{I} - \mathbf{C})^{-1}]'(\mathbf{I} - \mathbf{C}^{\ell})' + \boldsymbol{\Sigma}(0)(\mathbf{C}^{\ell})'.$$

On account of $\boldsymbol{\omega} = (\mathbf{I} - \mathbf{C})\boldsymbol{\sigma}$, it follows that

$$\boldsymbol{\Gamma}(\ell) = \boldsymbol{\Gamma}(0)(\mathbf{C}^{\ell})'.$$

Applying the vec operator to both side of the above equation yields eq. (17) as claimed. ■

Proof. (**of Theorem 3**) Rewrite $|\mathbf{r}_t|^{\wedge\boldsymbol{\delta}}$ in terms of deviations from the mean (see eqs. (4) and (12)):

$$|\mathbf{r}_t|^{\wedge\boldsymbol{\delta}} - \mathbf{r} = |\mathbf{Z}_t|^{\wedge\boldsymbol{\delta}}\left(\boldsymbol{\sigma}_t^{\wedge\boldsymbol{\delta}} - \boldsymbol{\sigma}\right) + \left(|\mathbf{Z}_t|^{\wedge\boldsymbol{\delta}} - \mathbf{Z}\right)\boldsymbol{\sigma} \text{ or}$$
$$\left(|\mathbf{r}_t|^{\wedge\boldsymbol{\delta}} - \mathbf{r}\right)' = (\boldsymbol{\sigma}_t^{\wedge\boldsymbol{\delta}} - \boldsymbol{\sigma})'\left(|\mathbf{Z}_t|^{\wedge\boldsymbol{\delta}}\right)' + \boldsymbol{\sigma}'\left(|\mathbf{Z}_t|^{\wedge\boldsymbol{\delta}} - \mathbf{Z}\right)'.$$

Multiplying $|\mathbf{r}_t|^{\wedge\boldsymbol{\delta}} - \mathbf{r}$ by its transpose, using the above expressions, taking expectations on both sides, and ignoring zero terms, it follows that the vectorization of $\boldsymbol{\Gamma}_r(0)$ is given by

$$\boldsymbol{\gamma}_r(0) = \mathbb{E}\left[\left(|\mathbf{Z}_t|^{\wedge\boldsymbol{\delta}}\right)^{\otimes 2}\right]\boldsymbol{\gamma}(0) + \widetilde{\mathbf{Z}}\boldsymbol{\sigma}^{\otimes 2}.$$

Applying eq. (16) to the above expression of $\boldsymbol{\gamma}_r(0)$, eq. (18) follows (the proof of eq. (19) is similar to the proof of eq. (18) and, thus it is omitted) and the proof is complete. ■

B APPENDIX: Dow Jones Graphs

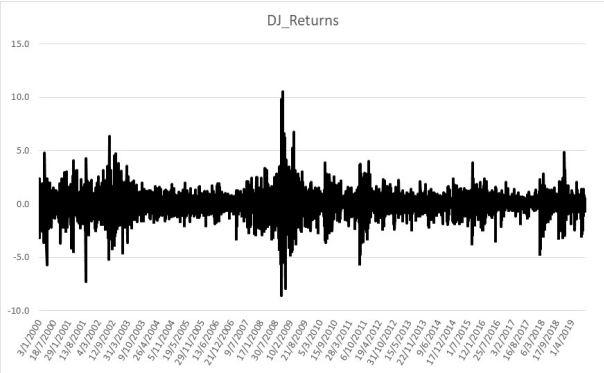

Figure A.1. Dow Jones Close-to-close Returns

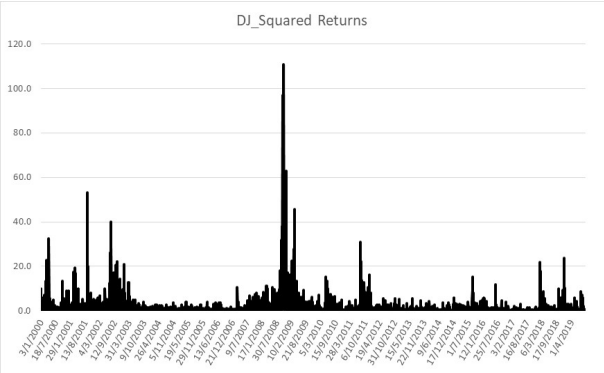

Figure A.2. Dow Jones Squared Returns

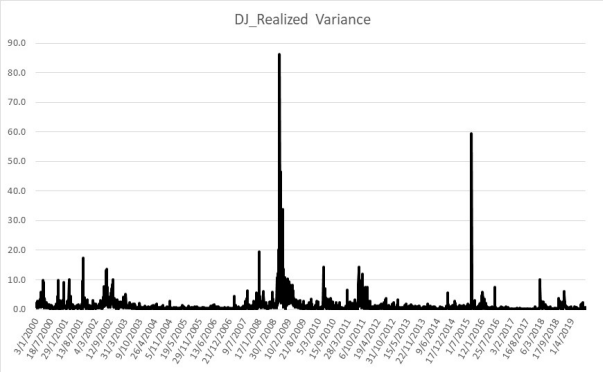

Figure A.3. Dow Jones Realized Variance

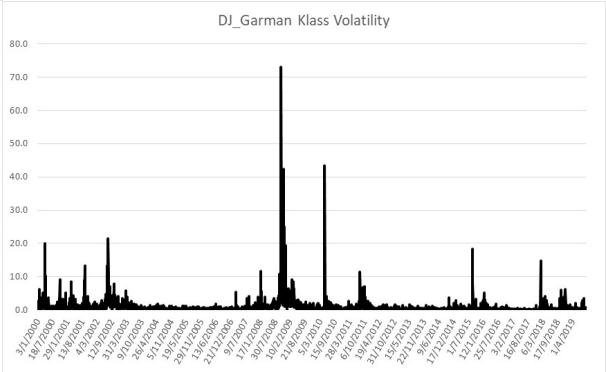

Figure A.4. Dow Jones Garman Klass Volatility

C APPENDIX: 3D-Benchmark Model Results

Table A.1. The 3D-Benchmark HEAVY model

	DJ	KOSPI	CAC	AORD	IPC
Panel A: Stock Returns, HEAVY-r					
$(1-\beta_r L)\sigma^2_{rt} = \omega_r + \alpha_{rR}L(RM_t) + \alpha_{rg}L(GK_t)$					
β_r	0.68 (17.59)***	0.67 (10.81)***	0.44 (7.65)***	0.77 (25.67)***	0.91 (61.24)***
α_{rR}	0.18 (3.36)***	0.40 (2.99)***	0.76 (6.66)***	0.28 (4.48)***	0.07 (6.78)***
α_{rg}	0.23 (4.41)***	0.23 (1.86)*	0.06 (3.52)***	0.13 (2.26)**	0.20 (7.21)***
Q_{12}	16.89 [0.15]	11.83 [0.46]	12.19 [0.43]	15.27 [0.23]	16.90 [0.15]
SBT	3.13 [0.00]	2.53 [0.01]	2.35 [0.02]	2.59 [0.01]	4.60 [0.00]
lnL	−6315.85	−7579.14	−7757.28	−5721.07	−7398.91
Panel B: Realized Measure, HEAVY-R					
$(1-\beta_R L)\sigma^2_{Rt} = \omega_R + \alpha_{RR}L(RM_t) + \alpha_{Rg}L(GK_t)$					
β_R	0.58 (12.42)***	0.55 (13.81)***	0.57 (16.89)***	0.73 (28.21)***	0.67 (11.04)***
α_{RR}	0.31 (4.44)***	0.34 (8.33)***	0.36 (9.78)***	0.19 (7.20)***	0.26 (3.49)***
α_{Rg}	0.14 (4.18)***	0.11 (3.95)***	0.06 (2.88)***	0.09 (3.82)***	0.06 (2.66)***
Q_{12}	12.85 [0.38]	15.44 [0.22]	9.46 [0.66]	16.89 [0.15]	9.53 [0.48]
SBT	3.45 [0.00]	5.26 [0.00]	2.39 [0.02]	2.67 [0.01]	3.12 [0.00]
lnL	−5922.35	−6135.93	−6818.17	−4357.03	−5816.53
Panel C: GK volatility, HEAVY-g					
$(1-\beta_g L)\sigma^2_{gt} = \omega_g + \alpha_{gR}L(RM_t)$					
β_g	0.58 (12.13)***	0.50 (7.36)***	0.57 (13.46)***	0.75 (31.27)***	0.76 (14.33)***
α_{gR}	0.33 (7.67)***	0.46 (7.04)***	0.38 (9.84)***	0.20 (9.86)***	0.24 (4.44)***
Q_{12}	9.65 [0.65]	12.72 [0.24]	9.33 [0.67]	12.39 [0.26]	9.62 [0.66]
SBT	4.42 [0.00]	3.01 [0.00]	2.85 [0.00]	3.22 [0.00]	8.70 [0.00]
lnL	−5402.41	−6068.15	−6630.57	−3997.18	−6290.51

Notes: See notes in Table 4.

SUPPLEMENTARY APPENDIX to the paper entitled:

'A Three-Dimensional Asymmetric Power HEAVY Model'

S. Yfanti[†], G. Chortareas[‡], M. Karanasos[⋆], E. Noikokyris[⊛]

[†]*Loughborough University, UK;* [‡]*King's College London, UK;*

[⋆]*Brunel University London, UK;* [⊛]*Kingston University London, UK*

September 2020

A Long Memory Extension

A.1 Hyperbolic Formulation

In this Section, we extend the 3D-DAP-HEAVY framework by incorporating long memory. First, we present the most general hyperbolic (HY) specification (see, for example, in the context of a univariate GARCH model Davidson, 2004, Dark, 2005, 2010, and Schoffer, 2003):

$$\begin{aligned}
(1-\beta_r L)[(\sigma_{rt}^2)^{\frac{\delta_r}{2}} - \omega_r] &= A_r(L)(1+\gamma_{rr}s_t)(r_t^2)^{\frac{\delta_r}{2}} + (\alpha_{rR}+\gamma_{rR}s_{t-1})L(RM_t)^{\frac{\delta_R}{2}} + (\alpha_{rg}+\gamma_{rg}s_{t-1})L(GK_t)^{\frac{\delta_g}{2}},\\
(1-\beta_R L)[(\sigma_{Rt}^2)^{\frac{\delta_R}{2}} - \omega_R] &= A_R(L)(1+\gamma_{RR}s_t)(RM_t)^{\frac{\delta_R}{2}} + (\alpha_{Rr}+\gamma_{Rr}s_{t-1})L(r_t^2)^{\frac{\delta_r}{2}} + (\alpha_{Rg}+\gamma_{Rg}s_{t-1})L(GK_t)^{\frac{\delta_g}{2}},\\
(1-\beta_g L)[(\sigma_{gt}^2)^{\frac{\delta_g}{2}} - \omega_g] &= A_g(L)(1+\gamma_{gg}s_t)(GK_t)^{\frac{\delta_g}{2}} + (\alpha_{gR}+\gamma_{gR}s_{t-1})L(RM_t)^{\frac{\delta_R}{2}} + (\alpha_{gr}+\gamma_{gr}s_{t-1})L(r_t^2)^{\frac{\delta_r}{2}},
\end{aligned} \tag{1}$$

with

$$A_i(L) = (1-\beta_i L) - (1-\phi_i L)[(1-\zeta_i) + \zeta_i(1-L)^{d_i}],\ i = r, R, g,$$

where $|\phi_i| < 1$, d_i, is the fractional differencing parameter with $0 \leq d_i \leq 1$, and ζ_i, is the amplitude or hyperbolic parameter with $0 \leq \zeta_i \leq 1$. In other words, we have three long memory parameters, ϕ_i, ζ_i, and d_i. So, now the Heavy parameters are nine in total. Similarly, the Arch parameters are nine, and the Garman parameters as well.

If $\zeta_i = 0$ and $\phi_i - \beta_i = \alpha_{ii}$, the HYDAP specification reduces to the DAP ones (see eq. (3) in the main body of the paper), since in this case $A_i(L) = \alpha_{ii}L$.

The HY specification also nests the fractional integrated (FI) one (see, for example, Baillie et al., 1996, Tse, 1998, Karanasos et al., 2004, and Conrad and Karanasos, 2006) by imposing the restriction $\zeta_i = 1$. In this case $A_i(L)$ in eq. (1) becomes

$$A_i(L) = (1 - \beta_i L) - (1 - \phi_i L)(1 - L)^{d_i}.$$

Finally, note that the sufficient conditions of Dark (2005, 2010) for the non-negativity of the conditional variance of a HYAPARCH $(1, d_i, 1)$ specification are: $\omega_i > 0$, $\beta_i - \zeta_i d_i \leq \phi_i \leq \frac{2-d_i}{3}$ and $\zeta_i d_i(\phi_i - \frac{1-d_i}{2}) \leq \beta_i(\phi_i - \beta_i + \zeta_i d_i)$, $i = r, R, g$ (see also Conrad, 2010). When $\zeta_i = 1$ they reduce to the ones for the FIGARCH $(1, d_i, 1)$ model (see Bollerslev and Mikkelsen, 1996).

A.2 Long Memory Estimation Results

We further extend the HEAVY framework by incorporating long memory. For the returns and the GK volatility, the chosen specification is the FIDAP, whereas for the realized measure we select the HYDAP one (with the exception of KOSPI realized variance, where the HYCAP model is preferred). In all cases, the power terms are presented as fixed parameters since they are estimated separately using univariate models. Tables 1A-1C present the 3D-HYDAP-HEAVY results.

In the FIDAP specification for the returns (see Table 1A), d_r is close to 0.50 (around 0.38 to 0.45). In all cases, the Wald tests (available upon request) reject the null hypotheses of $d_r = 0$ or 1. The other two long memory parameters, ϕ_r and the hyperbolic one, ζ_r, were insignificant and, therefore, they were excluded. The own and Garman asymmetry parameters are significant with estimated values $\gamma_{rr} \in [0.33, 0.50]$ and $\gamma_{rg} \in [0.15, 0.19]$, respectively. The Heavy parameter, α_{rR}, is significant as well and with estimated values between 0.06 and 0.12. In other words, the lagged values of all three powered variables (squared negative returns, realized measure and negative signed GK volatility) drive the model of the power transformed conditional variance of returns.

Table 1A. The 3D-HYDAP-HEAVY model

	DJ	KOSPI	CAC	AORD	IPC
Panel A: Stock Returns, FIDAP Specification					
$(1-\beta_r L)[(\sigma_{rt}^2)^{\frac{\delta_r}{2}} - \omega_r] =$					
$\left[(1-\beta_r L) - (1-L)^{d_r}\right](1+\gamma_{rr}s_t)(r_t^2)^{\frac{\delta_r}{2}} +$					
$\alpha_{rR}L(RM_t)^{\frac{\delta_R}{2}} + \gamma_{rg}s_{t-1}L(GK_t)^{\frac{\delta_g}{2}}$					
β_r	0.38 (4.56)***	0.41 (5.83)***	0.37 (2.74)***	0.36 (4.78)***	0.32 (2.85)***
d_r	0.42 (2.75)***	0.45 (9.23)***	0.42 (5.25)***	0.40 (7.68)***	0.38 (7.68)***
α_{rR}	0.07 (4.91)***	0.12 (2.25)**	0.10 (2.99)***	0.07 (3.12)***	0.06 (5.01)***
γ_{rr}	0.50 (5.04)***	0.33 (5.00)***	0.48 (6.11)***	0.43 (7.24)***	0.35 (5.78)***
γ_{rg}	0.17 (3.43)***	0.19 (3.27)***	0.18 (3.26)***	0.15 (2.92)***	0.16 (2.95)***
δ_r	1.30	1.50	1.40	1.60	1.60
δ_R	1.10	1.20	1.10	1.30	1.00
δ_g	1.00	1.20	1.10	1.20	1.20
Q_{12}	14.80 [0.25]	12.49 [0.41]	12.56 [0.40]	18.19 [0.11]	12.58 [0.39]
SBT	1.09 [0.28]	0.21 [0.84]	0.26 [0.79]	0.72 [0.47]	0.85 [0.40]
lnL	−5337.06	−6584.66	−6785.68	−5277.31	−6330.71

Notes: The numbers in parentheses are t-statistics. ***, **, * denote significance at the 0.01, 0.05, 0.10 level, respectively. Q_{12} is the Box-Pierce Q-statistics on the standardized residuals with 12 lags. SBT denotes the Sign Bias test of Engle and Ng (1993). lnL denotes the log-likelihood value for each specification. The numbers in square brackets are p-values.

In the HYDAP specification for the realized measure (see Table 1B), there is strong evidence of hyperbolic memory as not only d_R but also ζ_R is significant, with estimated values $0.47-0.55$ and $0.66-0.90$, respectively, with the Wald tests (available upon request) always rejecting the null of either a FIDAP ($H_0 : \zeta_R = 1$) or a DAP formulation ($H_0 : \zeta_R = 0$). The own and the cross (Arch) asymmetric parameters, $\gamma_{RR} \in [0.18, 0.57]$ and $\gamma_{Rr} \in [0.06, 0.10]$, are also significant, as well as the Garman parameter, $\alpha_{Rg} \in [0.06, 0.15]$. Own asymmetries are insignificant and excluded in the Korean index only, where we statistically prefer a HYCAP specification. This means that the power transformed conditional variance of $\widetilde{RM}_t$ is significantly affected by the lagged values of all three powered variables: realized measure, GK

volatility and squared negative returns.

Table 1B. The 3D-HYDAP-HEAVY model

	DJ	KOSPI	CAC	AORD	IPC
Panel B: Realized Measure, HYDAP Specification					
$(1-\beta_R L)[(\sigma^2_{Rt})^{\frac{\delta_R}{2}} - \omega_R] =$					
$\gamma_{Rr} s_{t-1} L(r_t^2)^{\frac{\delta_r}{2}} + \alpha_{Rg} L(GK_t)^{\frac{\delta_g}{2}} +$					
$(1-\phi_R L)[(1-\zeta_R) + \zeta_R (1-L)^{d_R}](1+\gamma_{RR} s_t)(RM_t)^{\frac{\delta_R}{2}}$					
β_R	0.63 $(15.77)^{***}$	0.36 $(6.28)^{***}$	0.58 $(14.25)^{***}$	0.44 $(4.54)^{***}$	0.36 $(2.33)^{**}$
ϕ_{RR}	0.33 $(3.90)^{***}$	0.18 $(2.13)^{**}$	0.32 $(8.09)^{***}$	0.03 $(7.56)^{***}$	0.05 $(5.82)^{***}$
ζ_R	0.70 $(17.30)^{***}$	0.66 $(7.75)^{***}$	0.84 $(37.40)^{***}$	0.81 $(28.05)^{***}$	0.90 $(14.23)^{***}$
d_R	0.53 $(10.02)^{***}$	0.47 $(12.10)^{***}$	0.54 $(21.91)^{***}$	0.55 $(9.97)^{***}$	0.47 $(11.31)^{***}$
α_{Rg}	0.15 $(8.56)^{***}$	0.10 $(5.57)^{***}$	0.06 $(3.99)^{***}$	0.12 $(5.75)^{***}$	0.08 $(1.88)^{*}$
γ_{RR}	0.42 $(2.64)^{***}$		0.18 $(3.36)^{***}$	0.57 $(4.87)^{***}$	0.21 $(2.99)^{***}$
γ_{Rr}	0.10 $(8.80)^{***}$	0.06 $(11.46)^{***}$	0.07 $(11.33)^{***}$	0.07 $(6.78)^{***}$	0.06 $(3.61)^{***}$
δ_R	1.10	1.20	1.10	1.30	1.00
δ_r	1.30	1.50	1.40	1.60	1.60
δ_g	1.00	1.20	1.10	1.20	1.20
Q_{12}	14.97 [0.24]	14.61 [0.26]	15.55 [0.21]	14.95 [0.25]	13.50 [0.30]
SBT	0.30 [0.76]	1.03 [0.30]	0.37 [0.71]	1.05 [0.29]	0.82 [0.41]
lnL	−4261.79	−4341.16	−4853.86	−3550.86	−4767.10

Notes: See notes in Table 1A.

Similarly to the model for the returns, in the FIDAP specification for the GK volatility (see Table 1C), d_g is around 0.40 to 0.44, whereas the hyperbolic parameter was insignificant. The own (Garman) and the cross Heavy asymmetric parameters, $\gamma_{gg} \in [0.10, 0.22]$ and $\gamma_{gR} \in [0.06, 0.10]$, are also significant. However, the Arch asymmetric effect, γ_{gr}, was insignificant and excluded, with the direct effect from powered squared returns, α_{gr}, included. Therefore, the lagged values of all three powered variables, that is, the squared returns and the negative signed realized variance and GK volatility, drive the model of the power transformed conditional variance of the range-based measure.

Table 1C. The 3D-HYDAP-HEAVY model

	DJ	KOSPI	CAC	AORD	IPC
	Panel C: GK volatility, FIDAP Specification				
	$(1-\beta_g L)[(\sigma^2_{gt})^{\frac{\delta_g}{2}} - \omega_g] =$				
	$\alpha_{gr} L(r^2_t)^{\frac{\delta_r}{2}} + \gamma_{gR} s_{t-1}(RM_t)^{\frac{\delta_R}{2}} +$				
	$\left[(1-\beta_g L) - (1-L)^{d_g}\right](1+\gamma_{gg} s_t)(GK_t)^{\frac{\delta_g}{2}}$				
β_g	0.27 (3.49)***	0.26 (1.90)*	0.26 (1.93)**	0.34 (2.14)**	0.28 (4.76)***
d_g	0.41 (9.56)***	0.43 (16.27)***	0.40 (14.31)***	0.40 (7.72)***	0.44 (2.01)**
α_{gr}	0.02 (1.71)*	0.02 (2.26)**	0.02 (2.77)***	0.03 (3.20)***	0.05 (1.90)**
γ_{gg}	0.22 (4.96)***	0.15 (5.14)***	0.17 (3.46)***	0.12 (2.66)***	0.10 (2.84)***
γ_{gR}	0.10 (3.59)***	0.07 (2.68)***	0.10 (4.66)***	0.09 (3.38)***	0.06 (5.01)***
δ_g	1.00	1.20	1.10	1.20	1.20
δ_r	1.30	1.50	1.40	1.60	1.60
δ_R	1.10	1.20	1.10	1.30	1.00
Q_{12}	10.93 [0.54]	15.21 [0.23]	11.06 [0.52]	10.99 [0.53]	10.89 [0.56]
SBT	0.40 [0.69]	0.39 [0.70]	1.29 [0.20]	1.20 [0.23]	1.11 [0.27]
lnL	−4343.66	−5061.74	−5218.49	−3078.81	−5283.32

Notes: See notes in Table 1A.

All in all, our long memory extension of the asymmetric power specification demonstrates once more that all powered conditional variances receive the notable impact from the first lags of the three power transformed variables. We find that a fractionally integrated specification better fits the squared returns and the Garman-Klass volatility, whereas a hyperbolic type of memory is preferred for the realized measure. The long memory feature reinforces our main argument that the lagged values of the power transformations of all three aforementioned variables move the dynamics of the three powered conditional variances. The fractionally integrated (asymmetric power) model for the returns and the Garman-Klass volatility equations pools information across both low-frequency and high-frequency based volatility indicators. Similarly, the more richly parametrized hyperbolic process for the realized variance equation is bolstered with low-frequency information as well since the lagged value of the powered squared negative returns improves the in-sample performance of the model. Intriguingly, these results stand in sharp contrast to the benchmark HEAVY model, where the intra-daily realized measure is not affected by squared daily returns and the daily returns conditional variance is only determined by the lagged realized measure

and the lagged returns variance since the asymmetries from negative returns are completely neglected. Furthermore, the powers are estimated with the two-stage procedure same as the asymmetric power specification with similar δ_r, δ_R, and δ_g values common across the three volatility equations.

B Structural Breaks

Since we analyzed the superiority of our asymmetric power extensions for the HEAVY system, in this Section, we investigate the impact of structural changes (detected in the three power transformed time series used as dependent variables) on the Heavy, Arch and Garman estimated parameters. The time-varying behavior of these parameters can be significant around a financial crisis break, in particular, indicative of the crisis effects on the volatility pattern. As an alternative to the long memory specification, we incorporate structural break dummies in the 3D-DAP-HEAVY system. We first identify the structural breaks in the three volatility series for DJ, focusing mainly on the recent global financial crisis, and study their impact on the three-dimensional framework. The methodology in Bai and Perron (1998, 2003a,b) is employed to test for structural breaks. They address the problem of testing for multiple structural changes in a least squares context and under very general conditions on the data and the errors. In addition to testing for the presence of breaks, these statistics identify the number and location of multiple breaks. So, we identify the structural breaks in the three powered series (power transformations [PT] of squared returns, realized measure, and GK volatility, see Tables 5A-5C in the main body of the paper) with the Bai and Perron methodology (see Table 2 and Figures 1-3). We use the breaks identified in order to build the slope dummies for the various parameters. One break date for the recent financial crisis of 2007/08 is detected so that we can focus on the crisis effect. We also detect one break date before and one after the crisis.

Table 2. The break dates for Dow Jones

	1^{st} Break	2^{nd} Break	3^{rd} Break
r	28/04/2003	31/10/2007	30/11/2011
R	**06/08/2003**	**30/10/2007**	**20/12/2011**
g	06/08/2003	31/10/2007	20/12/2011

Notes: Bai & Perron breaks identification: Results selected from the repartition procedure for 1% significance level with 5 maximum number of breaks and 0.15 trimming parameter. Dates in bold indicate that the corresponding dummy coefficient is used in the 3D-DAP-HEAVY model.

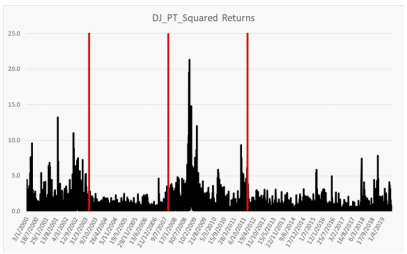

Figure 1. Dow Jones PT Squared Returns with Breaks

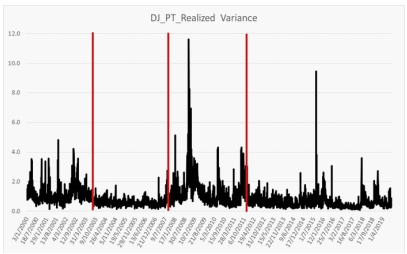

Figure 2. Dow Jones PT Realized Variance with Breaks

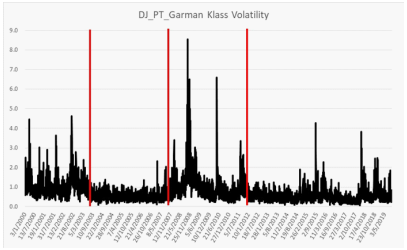

Figure 3. Dow Jones PT GK Volatility with Breaks

We present the estimation results for the DJ index in Table 3 (similar results for the other four indices available upon request), where we choose to use the 3 breaks of the power transformed realized variance series: (1) 06/08/2003: pre-crisis break, (2) 30/10/2007: crisis break and (3) 20/12/2011: post-crisis break. The three dummies multiplied by the respective Heavy, Arch and Garman variables (to construct the slope dummies) are defined as follows: $D_{i,t} = 0$, if $t < T_i$ and $D_{i,t} = 1$, if $t \geqslant T_i$, $i = (1), (2), (3)$ the three break dates. The 3D-DAP specification with structural breaks consists of the following equations (superscripts in parentheses indicate the break date):

$$\begin{aligned}(1-\beta_r L)(\sigma_{rt}^2)^{\frac{\delta_r}{2}} &= \omega_r + \\ (\gamma_{rr} + \gamma_{rr}^{(1)} D_{1,t-1} + \gamma_{rr}^{(2)} D_{2,t-1} + \gamma_{rr}^{(3)} D_{3,t-1}) s_{t-1} L(r_t^2)^{\frac{\delta_r}{2}} + \\ (\gamma_{rR} + \gamma_{rR}^{(1)} D_{1,t-1} + \gamma_{rR}^{(2)} D_{2,t-1} + \gamma_{rR}^{(3)} D_{3,t-1}) s_{t-1} L(RM_t)^{\frac{\delta_R}{2}} + \\ (\alpha_{rg} + \alpha_{rg}^{(1)} D_{1,t-1} + \alpha_{rg}^{(2)} D_{2,t-1} + \alpha_{rg}^{(3)} D_{3,t-1}) L(GK_t)^{\frac{\delta_g}{2}}\end{aligned} \tag{2}$$

$$\begin{aligned}(1-\beta_R L)(\sigma_{Rt}^2)^{\frac{\delta_R}{2}} &= \omega_R + [\alpha_{RR} + \alpha_{RR}^{(1)} D_{1,t-1} + \alpha_{RR}^{(2)} D_{2,t-1} + \alpha_{RR}^{(3)} D_{3,t-1} + \\ (\gamma_{RR} + \gamma_{RR}^{(1)} D_{1,t-1} + \gamma_{RR}^{(2)} D_{2,t-1} + \gamma_{RR}^{(3)} D_{3,t-1}) s_{t-1}] L(RM_t)^{\frac{\delta_R}{2}} + \\ (\gamma_{Rr} + \gamma_{Rr}^{(1)} D_{1,t-1} + \gamma_{Rr}^{(2)} D_{2,t-1} + \gamma_{Rr}^{(3)} D_{3,t-1}) s_{t-1} L(r_t^2)^{\frac{\delta_r}{2}} + \\ (\alpha_{Rg} + \alpha_{Rg}^{(1)} D_{1,t-1} + \alpha_{Rg}^{(2)} D_{2,t-1} + \alpha_{Rg}^{(3)} D_{3,t-1}) L(GK_t)^{\frac{\delta_g}{2}}\end{aligned} \tag{3}$$

$$\begin{aligned}(1-\beta_g L)(\sigma_{gt}^2)^{\frac{\delta_g}{2}} &= \omega_g + \\ (\gamma_{gg} + \gamma_{gg}^{(1)} D_{1,t-1} + \gamma_{gg}^{(2)} D_{2,t-1} + \gamma_{gg}^{(3)} D_{3,t-1}) s_{t-1} L(GK_t)^{\frac{\delta_g}{2}} + \\ (\alpha_{gR} + \alpha_{gR}^{(1)} D_{1,t-1} + \alpha_{gR}^{(2)} D_{2,t-1} + \alpha_{gR}^{(3)} D_{3,t-1}) L(RM_t)^{\frac{\delta_R}{2}} + \\ (\gamma_{gr} + \gamma_{gr}^{(1)} D_{1,t-1} + \gamma_{gr}^{(2)} D_{2,t-1} + \gamma_{gr}^{(3)} D_{3,t-1}) s_{t-1} L(r_t^2)^{\frac{\delta_r}{2}},\end{aligned} \tag{4}$$

We firstly apply the slope dummies in the Heavy, Arch, and Garman parameters of the DAP-HEAVY-r equation (see Panel A). In the returns equation, we estimate three different specifications with breaks:

the first (I) with the slope dummies on the cross Garman parameter, α_{rg}, the second (II) with the slope dummies on the own asymmetry (Arch) parameter, γ_{rr}, and the third (III) on the cross asymmetry (Heavy) parameter, γ_{rR}. All parameters increase with the crisis dummy and decrease with the pre- and post-crisis breaks. Regarding the realized measure equation (see Panel B), the Heavy impact, as captured by the Heavy parameter α_{RR}, and the own asymmetry γ_{RR}, the Arch asymmetric influence (captured by γ_{Rr}), and the Garman effect (α_{Rg}), all fall pre- and post-crisis and rise with the crisis break (specifications: I, II, III,IV). Finally, in the GK equation (Panel C), the own and the cross Arch asymmetries, γ_{gg} and γ_{gr}, and the Heavy impact, α_{gR}, increase during crisis and decrease during the pre- and post-crisis periods (specifications: I, II, III).

Table 3. The 3D-DAP-HEAVY model with structural breaks for Dow Jones

Panel A: Stock Returns								
I	β_r	α_{rg}	$\alpha_{rg}^{(1)}$	$\alpha_{rg}^{(2)}$	$\alpha_{rg}^{(3)}$	γ_{rr}	γ_{rR}	
	0.80 $(41.55)^{***}$	0.12 $(4.71)^{***}$	−0.04 $(-3.41)^{***}$	0.04 $(3.15)^{***}$	−0.03 $(-2.41)^{**}$	0.08 $(4.75)^{***}$	0.11 $(5.06)^{***}$	
II	β_r	α_{rg}	γ_{rr}	$\gamma_{rr}^{(1)}$	$\gamma_{rr}^{(2)}$	$\gamma_{rr}^{(3)}$	γ_{rR}	
	0.81 $(44.92)^{***}$	0.10 $(4.27)^{***}$	0.09 $(4.37)^{***}$	−0.05 $(-2.63)^{***}$	0.07 $(3.33)^{***}$	−0.03 $(-1.86)^{*}$	0.10 $(4.85)^{***}$	
III	β_r	α_{rg}	γ_{rr}	γ_{rR}	$\gamma_{rR}^{(1)}$	$\gamma_{rR}^{(2)}$	$\gamma_{rR}^{(3)}$	
	0.81 $(44.74)^{***}$	0.10 $(4.22)^{***}$	0.08 $(4.74)^{***}$	0.13 $(5.08)^{***}$	−0.05 $(-2.81)^{***}$	0.05 $(2.95)^{***}$	−0.04 $(-2.22)^{**}$	
Panel B: Realized Measure								
I	β_R	α_{RR}	$\alpha_{RR}^{(1)}$	$\alpha_{RR}^{(2)}$	$\alpha_{RR}^{(3)}$	α_{Rg}	γ_{RR}	γ_{Rr}
	0.71 $(39.24)^{***}$	0.10 $(5.12)^{***}$	−0.02 $(-3.22)^{***}$	0.02 $(4.66)^{***}$	−0.03 $(-6.08)^{***}$	0.12 $(7.66)^{***}$	0.06 $(5.53)^{***}$	0.08 $(8.25)^{***}$
II	β_R	α_{RR}	α_{Rg}	$\alpha_{Rg}^{(1)}$	$\alpha_{Rg}^{(2)}$	$\alpha_{Rg}^{(3)}$	γ_{RR}	γ_{Rr}
	0.71 $(38.87)^{***}$	0.08 $(4.62)^{***}$	0.13 $(8.47)^{***}$	−0.02 $(-3.43)^{***}$	0.03 $(5.07)^{***}$	−0.04 $(-6.40)^{***}$	0.06 $(5.55)^{***}$	0.08 $(8.34)^{***}$
III	β_R	α_{RR}	α_{Rg}	γ_{RR}	$\gamma_{RR}^{(1)}$	$\gamma_{RR}^{(2)}$	$\gamma_{RR}^{(3)}$	γ_{Rr}
	0.71 $(40.47)^{***}$	0.09 $(4.70)^{***}$	0.13 $(8.04)^{***}$	0.06 $(5.11)^{***}$	−0.02 $(-1.79)^{*}$	0.04 $(3.70)^{***}$	−0.05 $(-4.69)^{***}$	0.08 $(8.15)^{***}$
IV	β_R	α_{RR}	α_{Rg}	γ_{RR}	γ_{Rr}	$\gamma_{Rr}^{(1)}$	$\gamma_{Rr}^{(2)}$	$\gamma_{Rr}^{(3)}$
	0.72 $(39.97)^{***}$	0.08 $(4.45)^{***}$	0.13 $(8.13)^{***}$	0.05 $(5.18)^{***}$	0.08 $(8.22)^{***}$	−0.01 $(-1.68)^{*}$	0.03 $(2.95)^{***}$	−0.04 $(-3.29)^{***}$
Panel C: GK volatility								
I	β_g	γ_{gg}	$\gamma_{gg}^{(1)}$	$\gamma_{gg}^{(2)}$	$\gamma_{gg}^{(3)}$	α_{gR}	γ_{gr}	
	0.77 $(35.21)^{***}$	0.11 $(9.13)^{***}$	−0.04 $(-4.13)^{***}$	0.02 $(2.25)^{**}$	−0.03 $(-3.83)^{***}$	0.09 $(6.75)^{***}$	0.05 $(6.83)^{***}$	
II	β_g	γ_{gg}	α_{gR}	$\alpha_{gR}^{(1)}$	$\alpha_{gR}^{(2)}$	$\alpha_{gR}^{(3)}$	γ_{gr}	
	0.76 $(34.40)^{***}$	0.08 $(8.38)^{***}$	0.11 $(7.23)^{***}$	−0.03 $(-5.19)^{***}$	0.02 $(3.29)^{***}$	−0.02 $(-5.54)^{***}$	0.06 $(7.13)^{***}$	
III	β_g	γ_{gg}	α_{gR}	γ_{gr}	$\gamma_{gr}^{(1)}$	$\gamma_{gr}^{(2)}$	$\gamma_{gr}^{(3)}$	
	0.77 $(34.94)^{***}$	0.08 $(7.96)^{***}$	0.10 $(6.77)^{***}$	0.08 $(8.14)^{***}$	−0.03 $(-3.64)^{***}$	0.01 $(1.70)^{*}$	−0.02 $(-2.25)^{**}$	
Powers δ_i								
	δ_r	δ_R	δ_g					
	1.30	1.10	1.00					

Notes: See notes in Table 1A.

All in all, we evidence consistently the same signs of the dummies coefficients across all specifications with Heavy, Arch, and Garman parameters. The dummy parameters corresponding to the 2003 and 2011 breaks are negative, whereas the ones for the 2007/08 crisis are positive.

References

[1] Bai, J., Perron, P., 1998. Estimating and testing linear models with multiple structural changes. Econometrica 66, 47-78.

[2] Bai, J., Perron, P., 2003a. Computation and analysis of multiple structural change models. Journal of Applied Econometrics 18, 1-22.

[3] Bai, J., Perron, P., 2003b. Critical values for multiple structural change tests. Econometrics Journal 6, 72-78.

[4] Baillie, R. T., Bollerslev, T., Mikkelsen, H.O., 1996. Fractionally integrated generalized autoregressive conditional heteroskedasticity. Journal of Econometrics 74, 3-30.

[5] Bollerslev, T., Mikkelsen, H.O., 1996. Modelling and pricing long memory in stock market volatility. Journal of Econometrics 73, 151-184.

[6] Conrad, C., 2010. Non-negativity conditions for the hyperbolic GARCH model. Journal of Econometrics 157, 441-457.

[7] Conrad, C., Karanasos, M., 2006. The impulse response function of the long memory GARCH model. Economics Letters 90, 34-41.

[8] Dark, J.G., 2005. Modelling the conditional density using a hyperbolic asymmetric power ARCH model. Mimeo, Monash University.

[9] Dark, J.G., 2010. Estimation of time varying skewness and kurtosis with an application to Value at Risk. Studies in Nonlinear Dynamics and Econometrics 14, Article 3.

[10] Davidson, J., 2004. Moment and memory properties of linear conditional heteroscedasticity models, and a new model. Journal of Business and Economic Statistics 22, 16-29.

[11] Karanasos, M., Psaradakis, Z., Sola, M., 2004. On the autocorrelation properties of long-memory GARCH processes. Journal of Time Series Analysis 25, 265-281.

[12] Schoffer, O., 2003. HY-A-PARCH: A stationary A-PARCH model with long memory. Mimeo, University of Dortmund.

[13] Tse, Y.K., 1998. The conditional heteroscedasticity of the yen–dollar exchange rate. Journal of Applied Econometrics 13, 49-55.

The Data Analytics for Finance and Macro (DAFM) Research Centre
Forecasting trends is more important now than it has ever been. Our quantitative financial and macroeconomic research helps central banks and statistical agencies better understand their markets. Having our base in central London means we can focus on issues that really matter to the City. Our emphasis on digitalisation and the use of big data analytics can help people understand economic behaviour and adapt to changes in the economy.

Find out more at kcl.ac.uk/dafm

KING'S BUSINESS SCHOOL

Data Analytics for Finance & Macro Research Centre